

## **ABSTRACT**

Title of Dissertation: SURFACE-MODIFIED MAGNETIC NANOPARTICLES FOR CELLULAR INTERACTIONS AND IMPROVED BIOLOGICAL APPLICATIONS

Darryl Nathaniel Williams, Doctor of Philosophy, 2004

Dissertation directed by: Professor Tracey R. Pulliam Holoman  
Department of Chemical Engineering

In order to enhance the utilization of magnetic nanoparticles in biological systems, it is important to develop a fundamental understanding of the interactions that take place between the two systems. Magnetic nanoparticles are of particular interest for applications such as transfection, biodetection, and targeted drug delivery to name a few. The goal of this research was to study the effect iron oxide nanoparticles have on cellular growth and function, as well as to improve the particles' stability and biocompatibility in aqueous and biological media. Particle synthesis consisted of producing magnetite using the Massart method. Composite iron oxide nanoparticles produced under combustion synthesis were also studied. Previous results indicated that the inorganic nanoparticles formed small aggregates in microbial growth media, thus influencing particle stability. To mitigate this problem, a stabilizing polymer known as gum arabic was tested to control particle size and prevent further agglomeration in aqueous and growth media.

Results showed that gum arabic greatly improved particle stability. Growth studies measured the influence of the nanoparticles on cell proliferation using both M9 and Luria Bertani media to track growth of *Escherichia coli* (*E. coli*) in minimal and rich growth conditions. In addition to *E. coli*, prostate carcinoma cells (cell line DU145) were cultured in the presence of the treated nanoparticles to determine whether gum arabic improved the uptake of the particles in mammalian cells. Fluorescent microscopy was incorporated to detect the location of the nanoparticles in or about the cells by labeling the gum arabic with fluorescein isothiocyanate (FITC). The results illustrate the potential use of gum arabic as a surface-modifying agent to improve magnetic particle stability, as well as to promote nanoparticle uptake by mammalian cell cultures.

# **Surface-modified Magnetic Nanoparticles for Cellular Interactions and Improved Biological Applications**

by

Darryl Nathaniel Williams

Dissertation Submitted to the Faculty of the Department of Chemical Engineering of the University of Maryland, College Park in partial fulfillment of the requirements of Doctor of Philosophy  
2004

Advisory Committee:

Assistant Professor Tracey R. Pulliam-Holoman (Chairman)  
Associate Professor Sheryl H. Ehrman (Co-Advisor)  
Professor William E. Bentley  
Professor Nam S. Wang  
Associate Professor Luz Martinez-Miranda  
Assistant Professor Otto C. Wilson, Jr



## **DEDICATION**

This dissertation is dedicated to the voices of inspiration that have guided me from childhood to adulthood. Especially to my grandmother, Bernice E. Lee, who set the foundation for higher education and who sacrificed unconditionally so that her children would go on to achieve great things. To my parents, Juan and Bobbie Williams, for their continuous prayers, support, and remarkable example of determination and faithfulness. To my sisters, Juandria and Lacia, for believing in me. To my godfamily, The Tatums, for being gracious enough to care for me as their son.

## ACKNOWLEDGEMENTS

I would like to thank my advisors, Dr. Tracey Pullium Holoman and Dr. Sheryl Ehrman, for their endless support and guidance. I would also like to thank my other committee members, Dr. William E. Bentley, Dr. Luz Martinez-Miranda, Dr. Otto C. Wilson, Jr., and Dr. Nam S. Wang for serving as members of my dissertation committee. Thank you to our collaborators at Howard University, Dr. Winston Anderson and his group, for the use of their facilities and their expert advice in cell biology.

I would like to thank the GEM Science and Engineering Consortium, the Sloan Foundation, and the GAANN Fellowship for financial support.

Many thanks go out to Dr. Holoman's and Dr. Ehrman's group members for their assistance and support. I would also like to thank Tim Mangel of the University of Maryland Laboratory for Biological Ultrastructure for taking the time to section my samples. They always came out perfectly.

And finally, to my family and friends for *always* being there for me.

## TABLE OF CONTENTS

CHAPTER 1 – INTRODUCTION.....	1
CHAPTER 2 – BACKGROUND.....	3
Magnetic properties.....	4
Nanoparticles.....	7
Biodistribution.....	8
Colloid stability.....	9
Polymers.....	10
Section 1.1 Synthesis of Inorganic Nanoparticles.....	11
Section 1.1.1 Iron oxide nanoparticle synthesis.....	11
Section 1.1.2 Iron oxide composite nanoparticle synthesis.....	12
Section 2.2 Size Distribution and Morphology.....	14
Section 2.2.1 Dynamic light scattering.....	14
Section 2.2.2 Transmission electron microscopy.....	16
Section 2.2.3 BET analysis.....	16
Section 2.2.4 X-ray diffraction.....	18
Section 3.3 Surface Modification and Characterization.....	19
Section 3.3.1 Tetramethylammonium hydroxide.....	19
Section 3.3.2 Gum arabic.....	19
Section 4.4 Magnetite Surface Characterization.....	24
Section 4.4.1 Thermogravimetric analysis.....	24
Section 4.4.2 FTIR.....	24
Section 4.4.3 Zeta potential.....	25
Section 4.4.4 Adsorption isotherm.....	27
Section 5.5 Growth Activity Studies.....	28
Section 5.5.1 <i>Escherichia coli</i> .....	28
Section 5.5.2 Mammalian cell cultures.....	29
Section 5.5.3 Fluorescent microscopy.....	32
Section 5.5.4 Transmission electron microscopy.....	33
CHAPTER 3 – EVALUATION OF MICROBIAL CELLULAR RESPONSE TO INORGANIC NANOPARTICLES.....	34
Section 1.0 Introduction.....	34
Section 2.0 Materials and Methods.....	36
Section 3.0 Results.....	39
Section 4.0 Conclusions.....	51
CHAPTER 4 – SURFACE MODIFICATION OF MAGNETIC NANOPARTICLES USING GUM ARABIC.....	52
Section 1.0 Introduction.....	52
Section 2.0 Materials and Methods.....	54
Section 3.0 Results.....	59

Section 4.0 Discussion.....	69
Section 5.0 Conclusions.....	70
CHAPTER 5 – GUM ARABIC MODIFIED MAGNETIC NANOPARTICLES: INFLUENCE ON PROSTATE CANCER CELLS IN VITRO.....	72
Section 1.0 Introduction.....	72
Section 2.0 Methods and Materials.....	75
Section 3.0 Results.....	78
Section 4.0 Discussion.....	85
Section 5.0 Conclusions.....	87
CHAPTER 6 – CONCLUSIONS.....	88
CHAPTER 7 – FUTURE WORK.....	91
APPENDIX.....	94
REFERENCES.....	96

## LIST OF TABLES

Table 1. Characteristics of the inorganic nanoparticles used in experimentation.....	37
--	----

## LIST OF FIGURES

### CHAPTER 2

- Figure 1. (after Pankhurst et al., *J. Phys. D.: Appl. Phys.*, 2003) Hypothetical magnetic responses associated with different classes of magnetic material ranging in size that have been injected into a blood vessel. Diamagnetic (DM), paramagnetic (PM), ferromagnetic (FM), and superparamagnetic (SPM).....6
- Figure 2. Reactor setup for synthesis of magnetite nanoparticles.....12
- Figure 3. TEM image of a flame-generated iron oxide composite nanoparticle.....13
- Figure 4. List of representative amino acids contained in the gum arabic molecule (after Islam et al., *Food Hydrocolloids*, 1997).....21
- Figure 5. Proposed structure of the gum arabic molecule (after Islam et al., *Food Hydrocolloids*, 1997).....21
- Figure 6. (after Islam et al.. *Food Hydrocolloids*, 1997).....22
- Figure 7. after Silver Colloids ([www.silver-colloids.com/Tutorials/Intro/pcs1.html](http://www.silver-colloids.com/Tutorials/Intro/pcs1.html)).....27
- Figure 8. A reaction mechanism for the attachment of APTS to magnetite surfaces (after Ma, *Colloids and Surfaces A*, 2003).....33

### CHAPTER 3

- Figure 1. TEM of a  $\text{SiO}_2/\gamma\text{-Fe}_2\text{O}_3$  particle generated in a premixed flame.....40
- Figure 2. TEM image of gold particles without PEG coating (Majetich).....41
- Figure 3. TEM image of silica nanoparticles.....42
- Figure 4. TEM micrograph of cross sections of *E. coli* grown with composite iron oxide nanoparticles.....43
- Figure 5. Results of DLS for silica in LB media showing that the nanoparticles agglomerate in solution.....45
- Figure 6. DLS measurement of silica/iron oxide particles in LB media.....46
- Figure 7. Growth curves of *E. coli* in the presence of silica/iron oxide nanoparticles...47

Figure 8. Growth curves for <i>E. coli</i> in the presence of silica nanoparticles.....	48
Figure 9. Growth curves of <i>E. coli</i> in the presence of PEG-coated gold nanoparticles...	49
Figure 10. Growth curves of <i>E. coli</i> in the presence of higher concentrations of composite iron oxide nanoparticles.....	50
 CHAPTER 4	
Figure 1a. TEM of untreated magnetite nanoparticles synthesized using the Massart method.....	60
Figure 1b. Magnetite nanoparticles co-precipitated with gum arabic. Evidence is seen of larger agglomerates compared to untreated particles.....	60
Figure 2. DLS results of GA-coated magnetite nanoparticles in deionized water and M9 minimal media. Small changes occur in the hydrodynamic radius of the samples in M9 media that might be attributed to associated ions in the media.....	61
Figure 3. DLS measurements in deionized water of untreated, coated, and co-precipitated samples taken over a 30 hour period. Measurements were recorded for a 9hr period on day 1, left over night, and recorded again for an additional 6hrs.....	62
Figure 4. TGA results for untreated nanoparticles, co-precipitated nanoparticles, coated nanoparticles, and gum arabic powder.....	63
Figure 5. TGA results from concentrations of GA ranging from 1 to 15 wt%. Each sample contained 0.01g magnetite nanoparticles in 5 ml of GA solution.....	64
Figure 6. Adsorption isotherm of GA with magnetite nanoparticles extracted from TGA data.....	65
Figure 7. FTIR spectra for untreated magnetite, magnetite coated with gum arabic, and plain gum arabic powder.....	66
Figure 8. X-ray diffraction pattern for synthesized magnetite nanoparticles.....	67
Figure 9. Zeta potential measurements comparing GA-coated magnetic nanoparticles with untreated nanoparticles. GA causes a shift to the left, indicating less negative surface charge.....	68
Figure 10. Reaction mechanism for attachment of GA onto iron oxide surfaces.....	69

CHAPTER 5

Figure 1. Image of prostate carcinoma cell cultured with untreated nanoparticles. There is no visible concentration of nanoparticles within the cell.....78

Figure 2a. Image of prostate carcinoma cell with gum arabic treated nanoparticles at the membrane surface and within cellular components (i.e. lysosomes, vacuoles). Cells were inoculated with the treated nanoparticles for 30 minutes.....79

Figure 2b. Image of prostate carcinoma section with treated nanoparticles throughout the cell taken at a lower magnification.....80

Figure 3a. Phase view of DU-145 cells grown on glass slides with fluorescently labeled gum arabic coated nanoparticles.....81

Figure 3b. Fluorescent image of DU-145 cells grown on a glass slide with FITC-labeled gum arabic coated nanoparticles.....82

Figure 4a. DAPI stained nuclei of DU-145 cells (controls) without surface treated nanoparticles.....83

Figure 4b. Prostate carcinoma cells inoculated for 30 minutes with TRITC-labeled nanoparticles coated with gum arabic. DAPI stained nuclei (blue) for cell viability and to differentiate between nuclei and the cytoplasm (red) containing the nanoparticles.....84

## CHAPTER 1- INTRODUCTION

Research concerning the interactions between inorganic nanoparticles and biological cells will enable new developments in nanobiotechnology to reach their fullest potential. An improved understanding can lead to the development of new sensing, diagnostic, and treatment capabilities, such as improved targeted drug delivery, gene therapy, magnetic resonance imaging (MRI) contrast agents and biological warfare agent detection (Byers et al. 1987; Chan and Nie 1998; Chouly et al. 1996; Couvreur et al. 1994; Leong et al. 2001b) Among the many research issues are concerns about the overall toxicity of nanoparticles in biological environments. Cytotoxicity is of major concern and will become increasingly so as the demand for nanoparticles grows with the development of more biological applications. Questions such as how and if nanoparticles harm biological environments, how persistent they may be, and to what degree they affect people, are all concerns. It is known that nanoparticles can transfect cells; however, what occurs inside and outside the cell is not well understood.

This study focuses on several issues involving nanoparticle/cell interactions. Nanoparticles, because of their size, are highly functional for a number of biological applications. Magnetic nanoparticles offer additional functionality due to their ability to respond to magnetic fields. Unfortunately, not all inorganic nanoparticles are solely biocompatible without the aid of a protective layer on the surface to serve as a buffer for cellular interactions. Because of this, many studies have focused on developing methods to treat nanoparticle surfaces to increase their overall biocompatibility. For example, dextran and polyethylene glycol (PEG) are two common, biocompatible polymers often used to treat nanoparticle surfaces. However, recent studies point to evidence that

indicates dextran is not as biocompatible as currently believed (Berry et al. 2003). As a result, there is a push for finding and developing new surface-modifying agents to treat nanoparticles.

Colloid stability is another important issue that dictates the fate of nanoparticles in aqueous and physiological solutions. Stability has been a major topic of study, and there is still much to be understood concerning the origin and nature of interparticle forces and how they affect coagulation in dilute dispersions. The stability and, more generally, the microstructure and the macroscopic states of dispersions are determined by kinetic and thermodynamic considerations. Thermodynamics dictates what the equilibrium state will be, whereas the kinetics determine if the equilibrium state will be reached and how quickly (Hiemenz and Rajagopalan 1997). Increasing particle stability will aid in further developments of advanced sensing, diagnostic, and treatment capabilities as well as biological warfare detection systems.

Specific objectives of this work were:

- Synthesis and characterization of iron oxide nanoparticles.
- Surface modification and characterization of nanoparticles with a stabilizing polymer and fluorophore (e.g. gum arabic, FITC).
- Fluorescent microscopy and TEM for detecting the location of nanoparticles in or about cells.
- Growth studies to pinpoint subtle changes in cell function.

This thesis, herein, presents using gum arabic for treating and stabilizing iron oxide dispersions. Its also demonstrates the potential use of the material for targeting certain cell types, particularly cancer cells.

## CHAPTER 2 - BACKGROUND

Nanotechnology is now poised to revolutionize the electronic, chemical and biotechnology industries, and biomedical fields. One of the most important aspects of this field is the preparation and development of functionalized nanoparticles.

This research is attractive to many industries that will eventually move further into the development of nanoparticles for various biological applications. In particular, the biotechnology sector will see a major transformation in processes such as drug delivery, diagnostics, and biosensing in the future due to the influence of nanomaterials.

An improved understanding of magnetic nanoparticles and biological cell interactions can lead to the development of new sensing, diagnostic, and treatment capabilities, such as improved targeted drug delivery, gene therapy, MRI contrast agents, and biological warfare detection (Byers et al. 1987; Chan and Nie 1998; Chouly et al. 1996; Couvreur et al. 1994; Leong et al. 2001b).

The goal of the research herein was to investigate a new method of surface modification for magnetic nanoparticles, and to study the interactions between the newly treated particles and various cell types (microbial and mammalian). Nanoparticles present a research challenge because little is known about how they behave in relation to microorganisms, particularly at the cellular level. Size is a prominent feature of nanoparticles because of their large surface area. Other parameters, such as density, molecular weight, and crystallinity largely influence their release and degradation properties, whereas surface characteristics such as hydrophilicity and hydrophobicity significantly influence the interactions with biological environments (Kreuter 1997).

Applications of magnetic nanoparticles can be seen throughout biomedicine and other biologically related fields. Their magnetic properties allow them to be exploited in the presence of a magnetic field and used to function in areas such as bioseparation, in which the particles are treated to target or bind to a specific biological entity and segregate it from other species. Other areas of known application include, but are not limited to, drug delivery, enhanced imaging for MRI, and hyperthermia which will be discussed in greater detail later on in this chapter. Before describing other applications, a brief discussion of some of the basic concepts of magnetism is needed to better support the use of magnetic nanoparticles to drive certain processes.

If a magnetic material is placed in a magnetic field of strength  $\mathbf{H}$ , the individual atomic moments in the material contribute to its overall response, the magnetic induction:

$$\mathbf{B} = \mu_0(\mathbf{H} + \mathbf{M}). \quad (1)$$

where  $\mu_0$  is the permeability of free space, and the magnetization  $\mathbf{M} = \mathbf{m}/V$  is the magnetic moment per unit volume, where  $\mathbf{m}$  is the magnetic moment on a volume  $V$  of the material. All materials are magnetic to a certain extent, with their response depending on their atomic structure and temperature. They may be conveniently classified in terms of their volumetric magnetic susceptibility,  $\chi$ , where

$$\mathbf{M} = \chi \mathbf{H}. \quad (2)$$

describes the magnetization induced in a material by  $\mathbf{H}$ . In SI, units  $\chi$  is dimensionless and both  $\mathbf{M}$  and  $\mathbf{H}$  are expressed in  $\text{A m}^{-1}$ . Most materials display little magnetism, and even then only in the presence of an applied field. These are classified as either paramagnetic or diamagnetic. However, some materials exhibit ordered magnetic states and are magnetic even without a field applied, and these are classified as ferromagnetic,

ferrimagnetic, and antiferromagnetic (prefix refers to the nature of the coupling interaction between the electrons within the material) (Morrish 2001).

The susceptibility in ordered materials depends not just on temperature, but also on  $H$ , which gives rise to the characteristic sigmoidal shape of the  $M-H$  curve, with  $M$  approaching a saturation value at large values of  $H$ . Moreover, in ferromagnetic and ferromagnetic materials hysteresis is commonly observed. This is the irreversibility in the magnetization process that is related to the pinning of magnetic domain walls at impurities or grain boundaries within the material, as well as intrinsic effects such as the magnetic anisotropy of the crystalline lattice. This gives rise to open  $M-H$  curves called hysteresis loops (Pankhurst et al. 2003).

The shapes of these loops are determined, in part, by particle size. In large particles (micron or more) there is a multi-domain ground state that leads to a narrow hysteresis loop since it takes relatively little field energy to make the domain walls move; while for smaller particles, there is a single domain ground state which leads to a broad hysteresis loop. For nanometer sized particles, superparamagnetism can be observed, where the magnetic moment of the particle as a whole is free to fluctuate in response to thermal energy, while individual atomic moments maintain their ordered state relative to each other. This leads to an anhysteretic, but sigmoidal  $M-H$  curve (Pankhurst et al. 2003). Figure 1 shows different magnetic field response curves and is an example of how magnetic particle of varying size might behave in the blood stream.

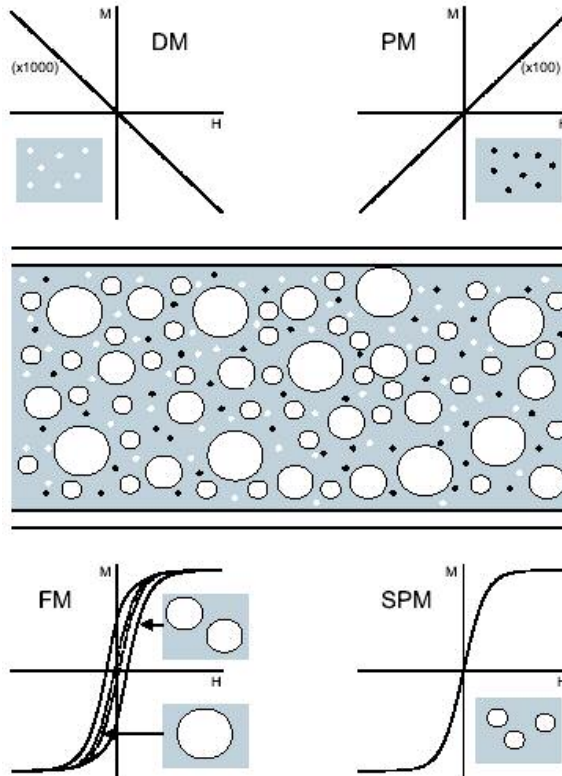


Figure 1. (after Pankhurst et al., *J. Phys. D.: Appl. Phys.*, 2003) Hypothetical magnetic responses associated with different classes of magnetic material ranging in size that have been injected into a blood vessel. Diamagnetic (DM), paramagnetic (PM), ferromagnetic (FM), and superparamagnetic (SPM).

Magnetic particles, such as maghemite and magnetite, have been in use since the mid-1970s in areas of bioscience and medicine. Their unique magnetic properties allow them to move in high magnetic field gradients making them useful in such areas as drug targeting and bioseparations. Magnetic particles generate a magnetic field and influence the local area around them making for excellent contrast agents in magnetic resonance imaging (MRI) (Shinkai 2002). Potential applications for biosensing techniques may also employ magnetic particles by selectively binding the particles to species of interest and mobilizing them under a magnetic field.

Nanoparticles exhibit their special drug delivery effects by direct interaction with their environment. Drug release may occur by desorption of the surface bound drug, diffusion through the nanoparticle matrix, or diffusion through the polymer wall (coated nanoparticles). The release mechanism, the diffusion coefficient, and the biodegradable rate are the main factors governing the drug release rate. Most importantly, the release rate of drugs from nanoparticles is strongly influenced by the biological environment (Kreuter 1997).

As mentioned previously, MRI technology can be improved by the use of magnetite nanoparticles. There are several reasons why magnetite nanoparticles can serve as more efficient contrast agents:

- 1) They have high magnetic moments and can therefore be used at very low concentrations.
- 2) When coated with hydrophilic polymers, magnetite can be coupled to targeted molecules like monoclonal antibodies, polypeptides, and hormones.

Recent studies are focused on the development of magnetite nanoparticles; however, there are wide range of preparation techniques and the physio-chemical properties of the particles differ greatly (Moreno 1992). These properties relate to the dimension of the particles and to the charge, hydrophobicity, and structural properties of the coating polymer. Magnetite nanoparticles retained as contrast agents for MRI must be superparamagnetic, nontoxic, and biodegradable (Chouly et al. 1996).

Additional studies have been conducted with the intention of finding efficient methods for producing these contrast agents, as well as altering their properties, giving them better pharmacokinetic and metabolic characteristics (Pouliquen et al. 1992). Other

parameters, such as biodistribution are functions of particle size, charge, and surface nature. Results from nanoparticle biodistribution studies give insight in to what preparation techniques are best suited for MRI of organs like the liver, lymph nodes, and assessment of tissue perfusion (Chouly et al. 1996).

An area of current research in nanobiotechnology is the use of nanoparticles as carriers for biological detection systems. Because of their size, these submicron materials are ideal for binding biological molecules that can recognize specific analytes, such as proteins, DNA, and viruses. The development of sensitive nonisotopic detection systems has substantially impacted many research areas, including DNA sequencing, clinical diagnostics, and fundamental molecular biology and opened new possibilities in ultrasensitive and automated biological assays (Chan and Nie 1998). Other uses for nanoparticles in biosensing are as fluorescent probes in biological staining and diagnostics. Compared with conventional fluorophores, some nanoparticles have narrow, tunable, symmetric emission spectrum and are photochemically stable (Bruchez et al. 1998).

When cells are exposed to chemical or physical stresses, they undergo alterations in the patterns of protein expression. For example, when some microbial cells are exposed to high temperatures, a set of heat shock proteins is transcriptionally upregulated. In addition to heat shock, other environmental factors, such as osmotic shock or nutrient limitation can play major roles in how cells respond to these stress factors. The question is how do certain types of microbial and mammalian cells respond in the presence of surface-modified iron oxide or iron oxide composite nanoparticles?

Colloid stability is another important factor that dictates the fate of nanoparticles in aqueous and physiological solutions. Stability has been a major topic of study, and there is still much to be understood concerning the origin and nature of interparticle forces and how they affect coagulation in dilute dispersions. The stability and, more generally, the microstructure and the macroscopic states of dispersions are determined by kinetic and thermodynamic considerations. Thermodynamics dictates what the equilibrium state will be, whereas the kinetics determine if the equilibrium state will be reached and how quickly (Hiemenz and Rajagopalan 1997).

Particle stability and theories of interaction forces between colloidal particles was developed by *Derjaguin-Landau-Verwey-Overbeek* (DLVO). They used this theory to study the dependence of colloid stability on the various parameters that determine the shapes and the magnitudes of interaction energies between particles. The DLVO theory provides a quantitative explanation for the fact that the addition of electrolyte into a colloid suspension can cause particles to undergo coagulation. For a particular salt, a fairly sharply defined concentration is needed to induce coagulation called the critical coagulation concentration (CCC). This theory can be summarized by the following statements:

1. The higher the potential at the surface of a particle (and throughout the double layer), the larger the repulsion between the particles.
2. The lower the concentration of indifferent electrolyte, the longer the distance from the surface before the repulsion drops significantly.
3. The larger the Hamaker constant,  $A$  (defines a net interaction of two bodies), the larger the attraction between macroscopic bodies.

The actual concentration of electrolyte at the CCC depends on: (a) the time allowed to elapse before the evaluation is made, (b) the uniformity, or the polydispersity of the sample, (c) the potential at the surface, (d) the value of  $A$ , and (e) the valence of the ions (Hiemenz and Rajagopalan 1997).

The role of polymers on colloid stability is more complicated than electrostatic stability due to low molecular weight electrolytes, such as KCl. According to the literature, if the added polymer moieties are polyelectrolytes, then there will be a combination of electrostatic effects as well as effects that arise from the polymeric nature of the additive; this combined effect is referred to as electrostatic stabilization. Even in the case of nonionic polymers, addition of the polymer to dispersions can promote stability or destabilize the dispersion, depending on the nature of the interactions between the polymer and the solvent, and between the polymer and the dispersed particles (Hiemenz and Rajagopalan 1997).

In the case of very low polymer concentrations, bridging flocculation may occur as a polymer chain forms bridges by adsorbing on more than one particle [Leong et al 2001b; Hiemenz, 1997 #69]. At higher concentrations of a polymer, “brushlike” layers can form on the particles. These brushes can be extended over sufficiently large distances to mask out the influence of van der Waals attraction between the particles, thereby imparting stability to the dispersion. This is known as steric stabilization; and for this mechanism to occur, the polymer molecules must be adsorbed or anchored on the particle surfaces. At moderate to high polymer concentrations, the “free” polymer chains in solution may cause depletion flocculation due to the influence of the exclusion of

polymer chains in the region between two particles when the particles are very close to one another (Hiemenz and Rajagopalan 1997).

## **Section 1.1 Synthesis of Inorganic Nanoparticles**

### **Section 1.1.1 Iron Oxide Nanoparticle Synthesis**

The preparation of magnetic nanoparticles has been an area of considerable study. Quantum size effects and the large surface area of magnetic nanoparticles dramatically change some of the magnetic properties, and the particles exhibit superparamagnetic phenomena because each particle is considered as a single magnetic domain. A difficulty related to the nature of magnetic fluids is that the nanoparticles, which have a large ratio of surface area to volume, tend to agglomerate in order to reduce their surface energy by strong magnetic dipole dipole attractions between particles. As a result, one of the main problems associated with producing stable magnetic fluid is prevention of agglomeration during the synthesis and coating process (Kim et al. 2001a).

In this study, magnetic nanoparticle synthesis will follow the Massart method. Figure 2 is a schematic representation of the reactor setup used for preparation of the magnetite nanoparticles in this research. The resulting particles are hydrophilic; negatively charged in alkaline medium and positively charged in acidic medium. Their stability depends on the nature and the concentration of the counterions. In an alkaline medium (pH>9), polarizing or highly charged cations, such as ammonium, alkaline, or alkaline-earth ions, give rise to flocculation, while low polarizing cations, such as tetramethylammonium (TMA) ion, favor solution stability (Massart 1981).

Mixing is also a major factor in the preparation of stable magnetic sols. Synthesis under vigorous mechanical stirring results in the formation of small particles by reducing the tendency to agglomerate. The use of nonmagnetic stirring is also important in preparing magnetic nanoparticles because of the influence of magnetism on particle formation.

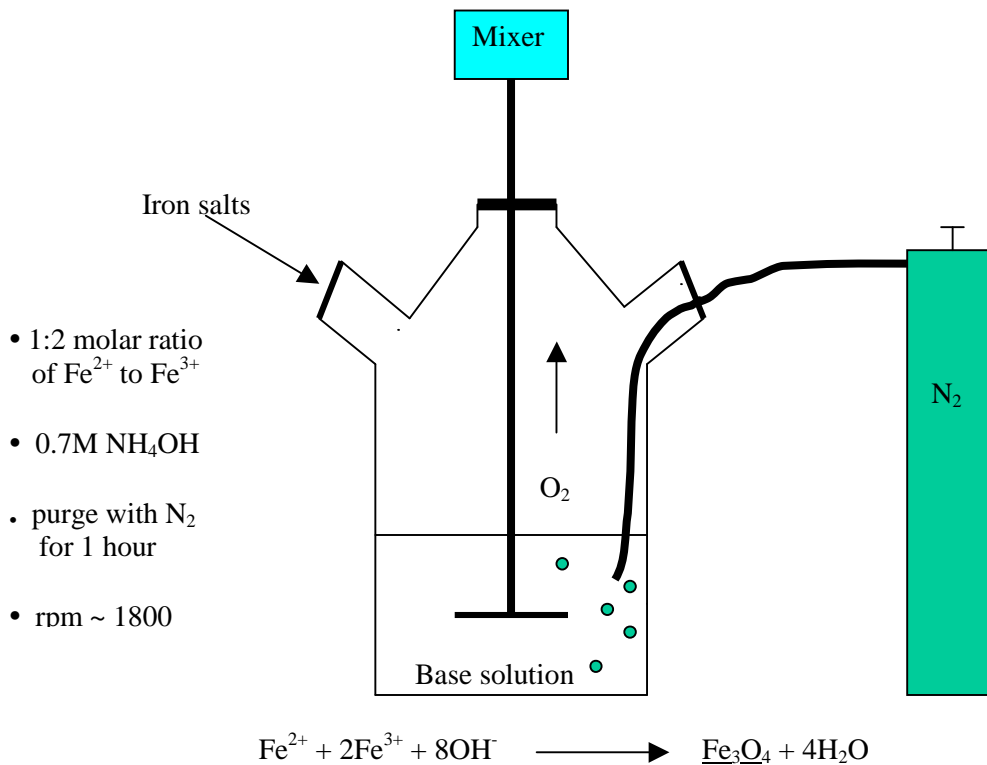


Figure 2. Diagram of the reactor setup used for synthesizing magnetite nanoparticles.

### Section 1.1.2 Iron Oxide Composite Nanoparticle Synthesis

Surface modification of magnetite nanoparticles is important not only for stability purposes, but also to increase their functionality. Finding a means to control size as well as maintaining stable sols is the subject of intense study. The flame generation process is the most widely used for the commercial production of inorganic oxide particles by

aerosol processes (Friedlander 1977). The aerosol precursor in the form of a vapor is mixed with oxygen and fed into a reactor chamber and burned. Inert gases and fuels, such as hydrogen or methane, may also be present. One studied in this research were silica and iron oxide composite nanoparticles that were flame-generated from iron pentacarbonyl and hexamethyldisiloxane in a premixed methane/oxygen/nitrogen flame (Ehrman et al. 1999). Each particle contains both  $\gamma\text{-Fe}_2\text{O}_3$  and silica, with a Fe to Si molar ratio of approximately 1:1. These “half-half” nanoparticles increase the functionality of the magnetic nanoparticle because of the highly reactive fused silica. The silica facilitates attachment of molecules such as fluorophores, biomaterials, or stabilizing agents. Figure 3 is a TEM of half-half iron oxide nanoparticles.

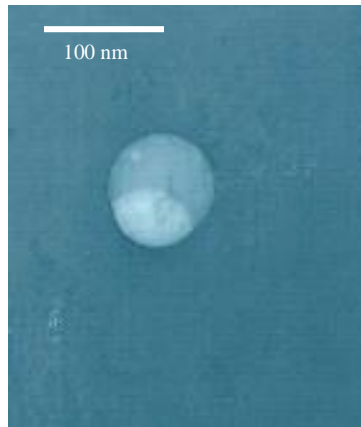


Figure 3. TEM image of a flame-generated iron oxide composite nanoparticle.

## Section 2.2 Size Determination and Morphology

### Section 2.2.1 Dynamic Light Scattering

One of the more common methods employed to characterize pharmaceutical colloids is dynamic light scattering (DLS). Analysis of the size distribution of the nanoparticles can be performed using a DLS autocorrelation tool known as PhotoCor-SP<sup>®</sup>. The photon correlation method is used to determine the velocity distributions of particles in suspension by measuring the dynamic fluctuations of the intensity of the scattered light. Disperse particles suspended in a liquid experience Brownian motion. This motion causes fluctuations of the local concentration of the particles resulting in local inhomogeneities of the refractive index. This leads to a Rayleigh scattering spectrum with linewidth  $\Gamma$  (defined as the half-width at half-maximum), which is proportional to the diffusion coefficient  $D$  of the particles:

$$\Gamma = D k^2, \quad (3)$$

where  $k = (4\pi n/\lambda)\sin(\Theta/2)$  is the refractive index,  $\lambda$  the laser wavelength, and  $\Theta$  the scattering angle. Assuming the particles to be spherical and non-interacting, one can obtain the mean radius  $r$  from the Stokes-Einstein equation

$$r = k_B T / 6\pi\eta D, \quad (4)$$

where  $k_B$  is Boltzmann's constant,  $T$  the temperature, and  $\eta$  the shear viscosity of the solvent.

Information can be extracted from the autocorrelation function of the scattered-light intensity (the simplest case being spherical, monodispersed, non-interacting particles in a dust free fluid with a characteristic decay time  $\tau_c$ , which is the inverse of the linewidth  $\Gamma$ ). The diffusion coefficient and either particle size or viscosity can be found

by fitting the measured correlation function to a single exponential decay (Yudin et al. 1997).

Two techniques exist for measuring the correlation function: heterodyning and homodyning. In heterodyne measurements, the scattered light is mixed coherently with a static light source at the incident wavelength and the static field is added to the scattered fields at the photodetector. Equation 4 relating the linewidth  $\Gamma$  to the diffusion coefficient  $D$  is applicable for heterodyne experiments. In homodyne measurements, the photodetector receives scattered light only. Homodyning is most suitable of large intensities (e.g near the critical point of a fluid or for colloid systems). For homodyne spectrum the relation between  $\Gamma$  and  $D$  is:

$$\Gamma = 2Dk^2. \quad (5)$$

The autocorrelation function  $G(\tau)$  of the scattering light as a function of the delay time  $\tau$  is written as

$$G(\tau) = b[1 + \varepsilon \exp(-\tau/\tau_c)], \quad (6)$$

where the baseline correlation level  $b$  is proportional to the total intensity  $I$ . The coefficient  $\varepsilon$  depends on the amount of stray light and the apertures in the system. The size  $r$  calculated from Equation 4 is referred to as the hydrodynamic radius. It may be larger than the actual radius of the bare particles because of the presence of layers of solvent, surfactant molecules, or (for charged particles) associated ions. The computer calculates the size distribution of suspended particles from the accumulated autocorrelation function of the intensity fluctuations by inversion of the following relationship (Yudin et al. 1997):

$$g_1(\tau) = \int G(\Gamma) e^{-\Gamma \tau} d\Gamma. \quad (7)$$

DLS measurements may be taken of the nanoparticles in microbial growth media and tell more about the behavior of the particles in various salt concentrations. As with many particles in the nanometer regime, the issue of colloidal stability plays a role with the introduction of salt. Nanoparticles can agglomerate in saline environments due to the reduction of the protective surface charge known as the electric double layer that surrounds the surface. With DLS, agglomeration can be observed for the uncoated nanoparticles and compared to the coated nanoparticles to test colloid stability.

### **Section 2.2.2 Transmission Electron Microscopy (TEM)**

Transmission electron microscopy (TEM) is a procedure that is used to characterize the morphology of materials such as nanoparticles. These instruments are used because of the limited image resolution in light microscopes imposed by the wavelength of visible light. Electrons have wave-like characteristics, with a wavelength substantially less than visible light. Since electrons are smaller than atoms, TEMs are capable of resolving atomic level detail. Samples are prepared for TEM imaging by inserting a TEM grid (copper coated with formvar) into dry or wet powder (usually dried overnight) using tweezers to hold the grid. The sample grid is then lightly tapped to remove any excess particles, and the grid is placed in the TEM for imaging. This procedure can be used to characterize the coated and uncoated magnetic particles.

### **Section 2.2.3 Surface Area and Particle Size Analysis using BET Method**

The Brunauer, Emmett, and Teller (BET) method begins with the assumption of localized adsorption. However, there is no limitation as to the number of layers of molecules that may be adsorbed, thus there is no saturation of the surface with increasing

pressure. In general, the derivation assumes that the rates of adsorption and desorption from each layer are equal at equilibrium and that adsorption or desorption can occur from a particular layer only if that layer is exposed (if no additional layers are on top of it) (Hiemenz and Rajagopalan 1997).

BET theory can be applied to measuring specific surface areas of material. With monolayer adsorption, the saturation limit can be related to the specific surface area of the adsorbant (nitrogen in most cases). The BET equation,

$$V/V_m = cx/(1-x)[1+(c-1)x]. \quad (7)$$

is used to determine the volume of the adsorbed gas that would cover the surface if the adsorption were limited to a monolayer.  $V_m$  is therefore defined as,

$$V_m = 1/(m+b). \quad (8)$$

where  $V_m$  equals the volume of gas that would be adsorbed if a monolayer were formed, and  $m$  is the slope and  $b$  is the intercept.  $V$  and  $V_m$  are typically expressed in cubic centimeters at STP per gram, yielding

$$V_m = (n/w)_{sat}(22,414 \text{ cm}^3 \text{ mole}^{-1}) = A_{sp}(22,414)/N_A\sigma^0. \quad (9)$$

where  $A_{sp}$  is the specific surface area,  $N_A$  is Avagadro's number, and  $\sigma^0$  is known unambiguously. For this value, it is assumed that the adsorbed material has the same density on the surface that it has in the bulk liquid at the same temperature, and to assume the molecules are close packed on the surface. In many cases,  $\sigma^0$  is evaluated for a particular adsorbate from independent measurements of  $V_m$  and  $A_{sp}$  (Hiemenz and Rajagopalan 1997).

#### Section 2.2.4 Determination of Crystalline Structure

X-ray powder diffraction is a method used to determine the crystal structure and analyze the phase of a particular material. Diffraction occurs as waves interact with a regular structure whose repeat distance is about the same as the wavelength. The phenomenon is common in the natural world, and occurs across a broad range of scales. X-rays have wavelengths on the order of a few angstroms, the same as typical interatomic distances in crystalline solids, which means X-rays can be diffracted from minerals that, by definition, are crystalline and have regularly repeating atomic structures .

When certain geometric requirements are met, X-rays scattered from a crystalline solid can constructively interfere, producing a diffracted beam. A diffraction pattern appears, and this diffraction pattern can be analyzed to determine various structural properties of a material in question. W. L. Bragg recognized a predictable relationship among several factors:

- 1) The distance between similar atomic planes in a mineral (the interatomic spacing) called the d-spacing and measured in angstroms.
- 2) The angle of diffraction called the theta angle and measured in degrees. For geometrical reasons the diffractometer measures an angle twice that of the theta angle,  $2\theta$ .
- 3) The wavelength of the incident X-radiation, symbolized by  $\lambda$  and measured in angstroms (equals  $1.54 \text{ \AA}$  for copper which is commonly used).

These relationships are expressed in an equation defining Bragg's law, and can be written as follows:

$$n\lambda = 2d(\sin\theta). \quad (10)$$

### **Section 3.3 Surface Modification and Characterization**

#### **Section 3.3.1 Tetramethylammonium hydroxide (TMA)**

Tetramethylammonium hydroxide (TMA) is a low polarizing cation that favors solution stability and is commonly used to stabilize and re-disperse iron oxide particles precipitated in solution. Flocculation is reversible: upon substitution of the flocculating counterion in the precipitate by a more suitable one, the precipitate is re-dispersable. For example, if sodium hydroxide is used for precipitation of the magnetite, the  $\text{Na}^+$  cation can be exchanged with  $\text{NH}_4^+$  cation by stirring the precipitate with an ammonia-based buffer. Elimination of the flocculating  $\text{NH}_4^+$  counter-cation through its conversion into neutral  $\text{NH}_3$  ammonia by TMA then allows the peptization of the precipitate (Massart 1981). TMA is a highly basic (pH~14) solution significantly limiting its ability to serve as a stabilizing agent for biological applications.

#### **Section 3.3.2 Gum Arabic**

In this study, a new way of coating and synthesizing magnetic particles is introduced using a natural polymer known as gum arabic. To date, the use of gum arabic as a stabilizer of magnetic nanoparticles has not been investigated. Gum arabic (GA) is

the oldest and best known of all the tree gum exudates and has been used as an article of commerce for more than 5000 years. There is evidence that the ancient Egyptians used this material as an adhesive for mineral pigments in paints and for the flaxen wrappings used to embalm mummies (Islam et al. 1997). Today, this natural gum is widely used in the confectioneries and soft drink industries. Its ability to emulsify and stabilize flavoring oil dispersed in aqueous medium has no equal in the soft drink industries given the cost. Given its excellent emulsifying property, its surface active property may also be beneficial for processing solid-liquid dispersions. At present, little is known about what role GA plays in solid-liquid dispersions (Moreno 1992).

GA is unique in that it is made up of two major fractions: a high molecular weight (Mw) glycoprotein containing 90% carbohydrate and a lower Mw heterogeneous polysaccharide. In nature, GA is found as a mixed calcium, magnesium, and potassium salt of a polysaccharide acid (arabic acid). It is composed of six carbohydrate moieties and has a small portion of protein as the integral part of the structure. The macromolecules have a Mw ranging from  $3 \times 10^5$  to 2 million. Despite its high Mw, GA forms a relatively low viscosity solution even at concentrations as high as 50wt% (Leong et al. 2001b).

Various studies have been performed to characterize the properties of GA, including Smith degradations along with gel permeation chromatography. The protein and carbohydrate components were analyzed at each stage, and it was determined that the protein was present in all of the degradation products, although the sugar:protein ratio was higher at the core of the molecule (11:1) than the periphery (40:1).

A. senegal	
Asp	91
Hyp	256
Thr	72
Ser	144
Glu	36
Pro	64
Gly	53
Ala	28
Cys	3
Val	35
Met	2
Ile	11
Leu	70
Tyr	13
Phe	30
His	52
Lys	27
Arg	15
% N	0.365

Figure 4. List of representative amino acids contained in the gum arabic molecule (after Islam et al., *Food Hydrocolloids*, 1997).

Other studies indicate that GA is a kind of arabinogalactan –protein (AGP) complex, suggesting that the binding site is in a hydroxyproline-rich domain since deglycosylation using hydrofluoric acid and repeated periodate oxidation did not affect the interaction. The studies showed the presence of hydroxyproline, oligoarabinoside and serine-carbohydrate linkages (Fauconnier et al. 2000).

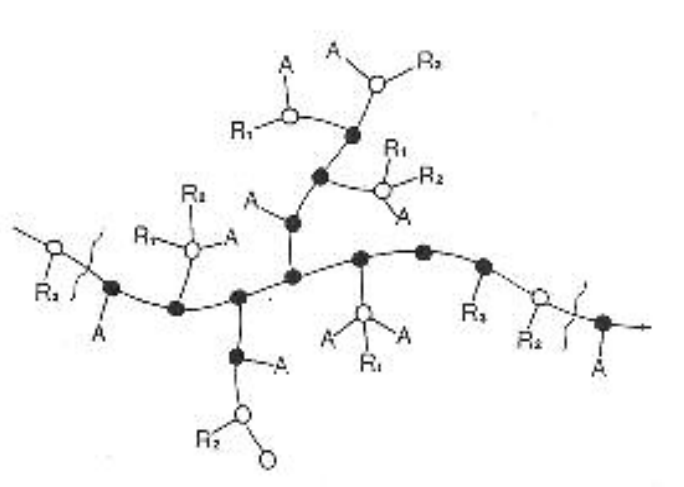


Figure 5. Proposed structure of the gum arabic molecule (after Islam et al., *Food Hydrocolloids*, 1997).

A profile of the molecular mass distribution of the gum by GPC monitoring the eluent by UV absorption at 214 nm resulted in chromatograms showing three or four peaks, indicating that the gum contains fractions of varying molecular mass. It has been suggested that the high molecular mass fraction, which represents ~ 30% of the total gum, is an AGP complex. These results have led to the suggestion that the gum has a

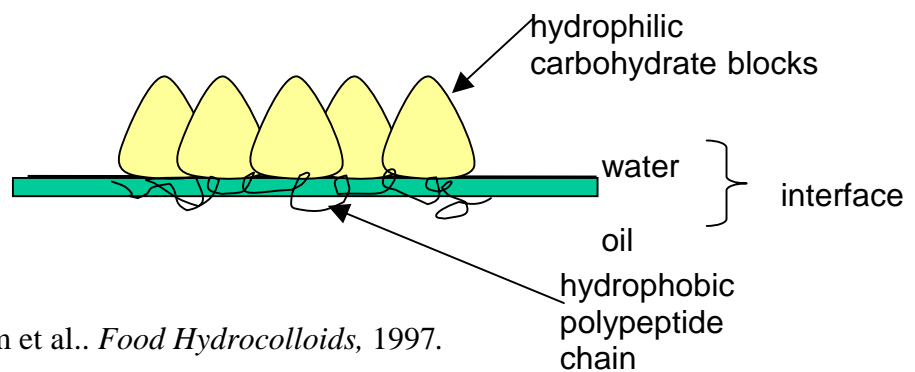


Figure 6. after Islam et al.. *Food Hydrocolloids*, 1997.

“waddle blossom” structure with a number of polysaccharide units linked to a common polypeptide chain as seen in Figure 6.

As mentioned previously, GA is used as an emulsifier in the encapsulation of flavor oils that may be spray dried for incorporation in dried food mixes, such as soups, cakes, etc., or in the manufacture of soft drinks. Investigations of rheological properties and emulsion stability show that it is the high molecular mass protein rich component that preferentially adsorbs at the oil-water interface. It has been postulated that the more hydrophobic polypeptide chain adsorbs to the surface of the oil droplets, while the

hydrophilic carbohydrate blocks attach to the chain protruding out into solution providing a strong steric barrier preventing droplet aggregation and coalescence (Islam et al. 1997).

GA is a molecule with positively and negatively charged functional groups. When adsorbed on a particle surface, like more conventional polyelectrolytes, GA may give rise to various non-DLVO surface forces, such as steric, bridging, and charged patch depending on the pH of the particle solution (Leong et al. 2001b). Bridging of particles occurs due to weak hydrogen bonds and van der Waals bonds. In cases using high molecular weight polyelectrolytes, such as those used in sedimentation applications, particles bridge by electrostatic attraction between unlike charges. Adsorbed strong polyelectrolyte at moderate surface coverage gives rise to charged patched force. This force is relatively weak compared to bridging and has the same magnitude as van der Waals.

Other studies have included using GA to stabilize individual carbon nanotubes in aqueous solutions. Single-wall carbon nanotubes pack into crystalline ropes that aggregate into tangled networks due to strong van der Waals attractions. Aggregation acts as an obstacle and diminishes the special properties of these nanotubes. To mitigate this problem, researchers have developed a simple way to treat the nanotubes to prevent them from forming aggregates using GA. Results show GA not only worked well as a stabilizing agent, but it also allowed the nanotubes to be dried in air, at ambient conditions, and redispersed in pure water in concentrations ranging from 0.5 wt% to 15 wt% (carbon nanotubes powder weight per water weight). The resulting suspensions were stable over months, and centrifugation (4500 rpm for 30 minutes) did not result in precipitation of the nanotubes (Bandyopadhyaya et al. 2001).

## **Section 4.4 Magnetite Surface Characterization**

### **Section 4.4.1 Thermogravimetric Analysis**

Thermogravimetric analysis (TGA) registers the constancy, loss, or gain in weight of a heated substance as a function of the temperature of that part of the furnace in which it is situated. If the heating cycle of the furnace is known, then the variation in weight as a function of time is also known. This method of analysis is useful in determining how much of a substance is adsorbed to a particular species. In this case, the change in weight of an untreated particle would be compared to the change in weight of a coated particle. By subtracting the two, the difference would then be the amount of coating adsorbed on the surface of the magnetite nanoparticles. TGA can assist in improving the optimization of the adsorption of stabilizing materials onto particle surfaces (Dural 1953).

### **Section 4.4.2 FTIR**

In infrared spectroscopy, adsorption in the infrared region results in changes in vibrational and rotational status of the molecules. The adsorption frequency depends on the vibrational frequency of the molecules, whereas the adsorption intensity depends on how effectively the infrared photon energy can be transmitted to the molecule, and this depends on the change in the dipole moment that occurs as a result of molecular vibration. As a consequence, a molecule will adsorb infrared light only if the adsorption causes a change in the dipole moment. Thus, all compounds except for elemental diatomic gases, such as N<sub>2</sub>, H<sub>2</sub>, and O<sub>2</sub>, have infrared spectra (Durig 1980).

Fourier transform infrared spectroscopy (FTIR) is a sensitive tool that allows for the characterization of materials by generating spectra based on intensity versus frequency (or wavelength) measurements converted from Fourier transform calculations. FTIR has high sensitivity because it is not limited by the amount of signal available at particular resolutions. This is because FTIR utilizes a beamsplitter that separates the incident beam into two right angles. One beam goes to a stationary mirror then back to the beamsplitter and the other goes to a moving mirror. The motion of the mirror makes the total path length variable versus that taken by the stationary mirror beam. When the two meet up again at the beamsplitter, they recombine, but the difference in path lengths creates constructive and destructive interference: an interferogram. The recombined beam passes through the sample. The sample absorbs all the different wavelengths characteristic of its spectrum, and this subtracts specific wavelengths from the interferogram. The detector reports variation in energy versus time for all wavelengths simultaneously. A laser beam of known wavelength and intensity is superimposed to provide a reference for the instrument operation (Durig 1980).

FTIR spectra are generated for both unmodified and modified magnetite. This technique will be important in identifying the difference between functional groups for particles coated with silica, particles treated with stabilizing agents, and particles left untreated. Functionalization of the particles can be improved once the surface chemistry is fully understood.

#### **Section 4.4.3 Zeta potential measurements**

The potential at the surface of shear for a particle is defined as the zeta potential. Derivations show that the zeta potential is the double-layer potential close to the particle

surface, and one of its applications is the measurement of surface charges of particle surfaces, such as nanoparticles. The liquid layer of a particle in suspension migrating in an electric field moves at the same velocity as the surface (shear surface). This shear surface occurs well within the double layer, likely at a location roughly equivalent to the Stern surface. Although the precise location of the surface of shear is unknown, it is assumed to be within a couple of molecular diameters of the actual particle surface for smooth particles. This “thickness” is associated with the zeta potential and defines the ion atmosphere near a surface (Hiemenz and Rajagopalan 1997).

The magnitude of the zeta potential gives an indication of the potential stability of a colloidal system. If all the particles have relatively large negative or positive zeta potentials, they will repel each other and create dispersion stability. If the particles have low zeta potential values, there is no force to prevent the particles from agglomerating and there is dispersion instability. A dividing line between stable and unstable aqueous dispersions is generally taken at either +30 or -30mV. Particles with zeta potentials more positive than +30mV are normally considered stable. Particles with zeta potentials more negative than -30mV are normally considered stable (Figure 7).

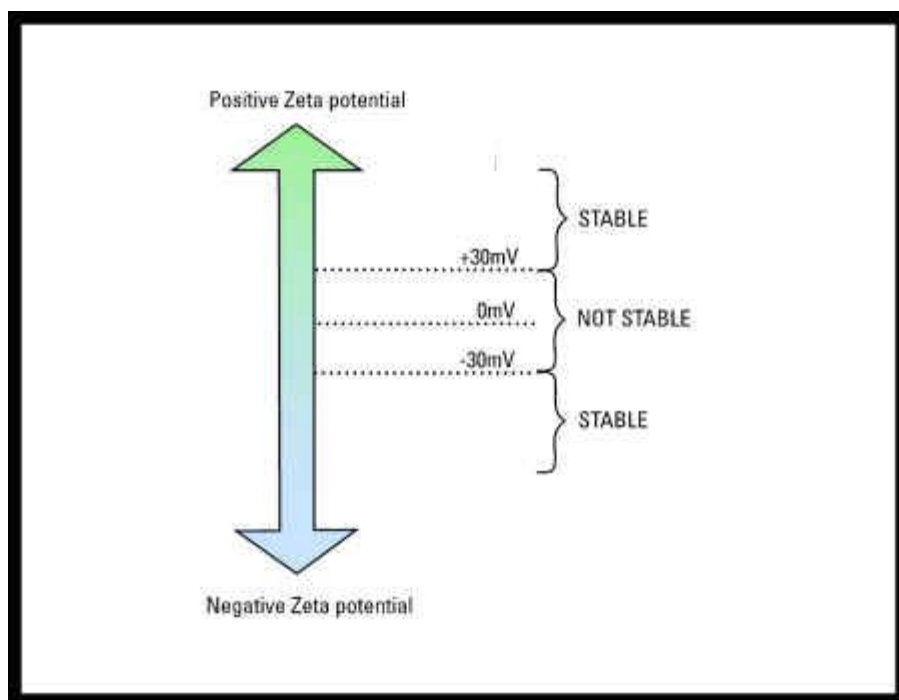


Figure 7. Taken from Silver Colloids ([www.silver-colloids.com/Tutorials/Intro/pcs1.html](http://www.silver-colloids.com/Tutorials/Intro/pcs1.html)).

#### Section 4.4.4 Adsorption Isotherm Studies

Characterizing the surface adsorption properties of materials is an important way to determine how well a particular adsorbate attaches to the surface of an adsorbent. If a dilute solution of a surface-active substance is brought in contact with a large adsorbing surface, then the adsorption will occur with a reduction in the concentration of the solution. From analytical data describing the concentration change in the solution as well as the known amount of solid and solution equilibrated, the amount of substance adsorbed can be determined per unit weight of adsorbing solid. These studies are generally performed at constant temperature and relate the amount of material adsorbed to the equilibrium concentration of the solution, resulting in what is known as the adsorption isotherm (Hiemenz and Rajagopalan 1997).

## **Section 5.5 GROWTH ACTIVITY STUDIES**

### **Section 5.5.1 Escherichia coli (*E. coli*)**

Currently, there has been little research done concerning the relationship between nanoparticles and microbial cells. Microbial cells are an attractive testing source because they are typically less particular about their environment than mammalian cells. In this study, *E. coli* serves as the model bacterium. *E. coli* is a bacterium that replicates very quickly at an optimal temperature of 37°C. It is a well-characterized microorganism and is widely used in biotechnology because it is easy to handle and use experimentally, hence a model bacterium. The response of *E. coli* to its physical environment is in no respect exceptional among bacteria. It is classified as a mesophile with respect to growth temperature and as a neutrophile with respect to pH range. Because of this, it grows over a mid range of temperatures, pH values, water activities, and pressure in which bacterial growth occurs.

*E. coli* was used to study the interactions between magnetite nanoparticles and microbial cells in minimal and rich growth media under batch conditions. The optical density versus time is recorded to measure the growth rate using a spectrophotometer set at 600nm. In previous cell/nanoparticle studies, *E. coli* was grown in Luria Bertani (LB) growth media that is rich in nutrients that provide an excellent source of food for rapid growth. To obtain accurate data concerning growth activity, it is more beneficial that the cells grow less quickly to track the growth process more efficiently. For this to occur, the cells need to be in media that has minimal nutrients which slows cell proliferation, hence the use of M9 minimal media. Another advantage associated with using M9 is that it is optically clear and does not contain amino acids that fluoresce, unlike LB media. This

makes it favorable for doing experiments, such as DLS or fluorescent microscopy, where the detection of particle distributions or fluorescence is sensitive to species that attenuate light.

Interactions between nanoparticles and microbial cells have not been well characterized. There have been studies conducted which applied DLVO (Derjaguin, Landau, Verwey, Overbeek) theory to describe bacterial adhesion in a wide range of applications, involving microbial adhesion on food processing equipment, biomaterial implants, bioreactor supports, etc. The microbial cell surface carries a net negative charge under most physiological conditions. It is a highly dynamic surface responding strongly to environmental changes through adsorption of ions and macromolecular components. Charges groups may associate or dissociate upon changes in pH or ionic strength of the suspending fluid, but also upon approach of a charges surface, either of another bacterium or a substratum. Inside the bacterial cell wall, charged groups are present and the distribution of these charges influences electric double layer interactions in bacterial adhesion (Poortinga et al. 2002). Given these facts about microbial cells, their interactions with surface-modified nanoparticles might be strongly influenced by the charge of the coating material and determine the difference between a specific or non-specific interaction.

### **Section 5.5.2 Mammalian Cell Cultures**

Presently, there has been much research into the use of nanoparticles to perform various biological tasks, but there is minimal evidence relating to the affect these submicron systems, themselves, have on cellular health and function. Questions about whether nanoparticles interfere with genetic or protein expression are medical concerns

that need to be addressed as nanoparticles become more commonplace due to the rise in research and development of these systems. Mammalian cells, such as myoblasts and macrophages, are examples of cultures used for various analyses because they are simple to grow. Mammalian cells have a longer growth cycle than microbial cells, therefore experiments can take days rather than hours. Growth studies for these cell types are performed by physically counting the cells to determine how well they grow with environmental changes.

Other cell types have been studied to determine their behavior in the presence of treated magnetic nanoparticles, such as cancer cells. Human mammary carcinoma cells and human ovarian tumor cells (HeLa cells) are often used in studies involving magnetic nanoparticles, particularly because they are simple to grow. Cancer cells, in general, are more robust than normal cells and this is believed to be caused by changes in a cell's DNA sequence, distinguishing it from a normal cell. Several factors are innate to cancer cells:

- 1) They and their progeny reproduce in defiance of the normal restraints on cell division.
- 2) They invade and colonize territories normally reserved for other cells.

It is this combination that makes cancers particularly dangerous (Alberts 2001)].

Treated magnetic nanoparticles, such as dextran-coated particles, are frequently used for MRI applications, but it has been observed that they do not present sufficient cellular uptake to enable cell tracking because of a relatively inefficient fluid phase endocytosis pathway (Berry and Curtis 2003). Because of this, other means of surface modification have been and are currently being explored to increase the uptake efficiency

of magnetic nanoparticles. This brings to question the fate of nanoparticles once they are administered in a biological environment, especially during intravenous administration.

After particles are injected into the bloodstream, they are rapidly coated by components of the circulation system, such as plasma proteins. This process is known as opsonization and leads to the particles being recognized by the body's major defense system, the reticulo-endothelial system (RES). The RES is the diffuse system of specialized cells that are phagocytic (i.e. engulf inert material) associated with the connective tissue framework of the liver, spleen, and lymph nodes. Macrophage cells play a critical role in the removal of opsonized particles. As a result, the application of nanoparticles *in vivo* or *ex vivo* requires surface modification that ensures particles are non-toxic, biocompatible, and stable to the RES (Berry and Curtis 2003).

Studies on different contrast agents have shown that biodistribution depends on the size, charge, and thickness of the coating material. Particles that have a largely hydrophobic surface are efficiently coated with plasma proteins and rapidly removed, whereas particles that are more hydrophilic can resist opsonization and are cleared more slowly (Gaur et al. 2000b). As mentioned previously, much of the literature available on cell response to iron oxide particles has focused on particles modified with dextran or starch-coated magnetite, both of which have shown no measurable toxicity index LD<sub>50</sub>. But surprisingly, several cases point to situations where dextran-magnetite particles caused areas of cell death, possibly due to the dextran shell being broken down yielding particle chains and aggregates that might influence cell processes (Berry et al. 2003). This being the case, other types of coatings need to be investigated to promote more stable, biocompatible nanoparticles.

### **Section 5.5.3 Fluorescent Microscopy**

Another form of surface modification is using a fluorescent dye to make the nanoparticles visible under ultraviolet (UV) light. This technique is an excellent way of physically observing the interactions of the nanoparticles with the cells. There are several methods for adsorbing fluorophores to particle surfaces, particularly on silica surfaces due to the reactive hydroxyl groups surrounding the surface. The procedure used to make these systems consists of two steps. First, the dye is chemically bound to a silane-coupling agent; and secondly, this coupling agent is used in the synthesis of colloidal silica by hydrolysis and condensation of tetraethyorthosilicate (TEOS) in mixtures of water, ammonia, and ethanol. The coupling agent commonly used is (3-aminopropyl) triethoxysilane (APTS). A fluorescent dye known as fluorescein isothiocyanate (FITC) is then covalently attached to the coupling agent APTS by an addition reaction of the amine group with the thioisocyanate group. Images of these particles can be taken using a confocal scanning laser microscope (van Blaaderen and Vrij 1992).

APTS, itself, can also bind to iron oxide nanoparticles, such as magnetite. A colloid-ethanol suspension diluted with water can be treated by ultrasonication under mild conditions, and then mixed with a small amount of APTS (Figure 8). Once this solution is prepared, it is mixed vigorously for several hours allowing the reaction to complete itself (Ma et al. 2003). At this point, one can attach a fluorophore (FITC, TRITC, etc.) to the coupling agent to create a fluorescently tagged nanoparticle.

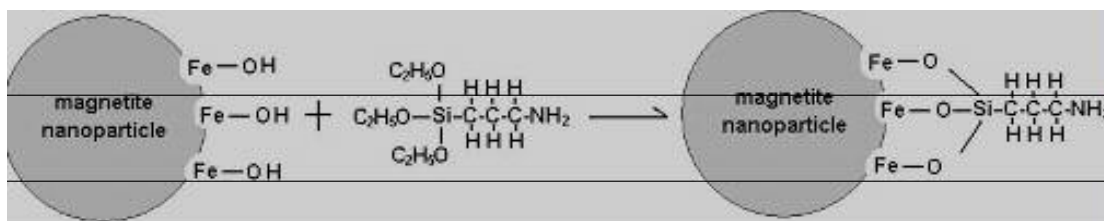


Figure 8. A reaction mechanism for the attachment of APTS to magnetite surfaces (after Ma, *Colloids and Surfaces A*, 2003).

#### Section 5.5.4 Transmission Electron Microscopy: Characterization of Cell/Magnetite Interactions

Using TEM to characterize cells is a method that would not require fluorescently tagged nanoparticles. Cell/particle interactions can be observed in much the same way as one would look for inclusion bodies in a cell. Samples of cells in the exponential and late exponential growth regions would be collected, centrifuged and suspended at room temperature in 0.1M sodium cacodylate (buffer) at pH 6.9 with 4% glutaraldehyde and 10mM CaCl<sub>2</sub>. The cell pellets are then washed again with 0.1M sodium cacodylate buffer, postfixed in 0.1M sodium cacodylate buffer containing 1% OsO<sub>4</sub> and 10mM CaCl<sub>2</sub> at pH 6.9 and room temperature. They are then rinsed in buffer and double distilled water, dehydrated in a series of ethanol and propylene oxide immersions, and embedded in Epon 812 resin. A diamond knife is used to section the embedded cells. The sections are poststained with 2.5% aqueous uranyl acetate and 0.2% aqueous lead citrate. TEM micrographs can then be obtained.

## CHAPTER 3 - EVALUATION OF MICROBIAL CELLULAR RESPONSE TO INORGANIC NANOPARTICLES

### Abstract

In order to enhance the utilization of inorganic nanoparticles in biological systems, it is important to develop a fundamental understanding of the influence they have on cellular health and function. Experiments were conducted to test silica, silica/iron oxide, and gold nanoparticles for their effects on the growth and activity of *Escherichia coli* (*E. coli*). Transmission electron microscopy (TEM) and dynamic light scattering (DLS) were used to characterize the morphology and quantify size distribution of the nanoparticles, respectively. TEM was also used to verify the interactions between composite iron oxide nanoparticles and *E. coli*. The results from DLS indicated that the inorganic nanoparticles formed small aggregates in the growth media. Growth studies were also performed to measure the influence of the nanoparticles on cell proliferation at varying concentrations. The growth curves and TEM micrographs of *E. coli* in media containing the nanoparticles showed no overt signs of toxicity.

### 1. Introduction

Research concerning the impact of inorganic nanoparticles on cellular health will enable new developments in nanobiotechnology to reach their fullest potential. An improved understanding of nanoparticles and biological cell interactions can lead to the development of new sensing, diagnostic, and treatment capabilities, such as improved targeted drug delivery, gene therapy, magnetic resonance imaging (MRI) contrast agents,

and biological warfare agent detection (Chan and Nie 1998; Chouly et al. 1996; Couvreur et al. 1994; Douglas et al. 1987; Pouliquen et al. 1992).

Cytotoxicity is of major concern and will become increasingly so as the demand for nanoparticles grows with the development of more biological applications. Questions, such as how and if nanoparticles harm biological environments, how persistent they may be, and to what degree they affect people are all concerns. It is known that nanoparticles can transfect cells; however, responses to nanoparticles inside and outside of cells are unknown.

The goal of the research presented here is to investigate how nanoparticles interact with microbial cells, and what affect nanoparticles have on their growth process. Nanoparticles present a research challenge because little is known about how they behave in relation to microorganisms, particularly at the cellular level. The colloidal behavior of the inorganic nanoparticles in the microbial growth media was investigated to determine the stability of these systems in saline environments.

Three types of nanoparticles were used to conduct this study: silica, silica/iron oxide, and gold. The silica/iron oxide nanoparticles are important because of their magnetic properties. They could potentially be used for medical applications, such as MRI and targeted drug delivery applications. Another application would be to use them as biological sensors. Being that they are composites, the silica portion of the nanoparticle can be functionalized to attract various biological elements while the iron oxide portion can provide mobility under the presence of a magnetic field.

Gold nanoparticles are employed in multiple applications involving biological systems. Gold has exceptional binding properties, and this makes it attractive for

attaching ligands to enhance various biomolecular interactions. These nanoparticles also exhibit an intense color in visible region for spectroscopic detection and also great contrast for electron microscopic imaging (Lin et al. 2002). Despite all of these applications for gold nanoparticles, there is still little knowledge as to how these colloid systems affect microbial environments. Silica nanoparticles are favorable because they are inexpensive, easy to produce, and have surface hydroxide groups that make them easy to functionalize.

## **2. Materials and Methods**

### *2.1 Inorganic Nanoparticles*

Table 1 gives the specifications for each type of nanoparticle (silica, silica/iron oxide, and gold) used in this study. The silica nanoparticles were made by base catalyzed hydrolysis of TEOS (Byers et al. 1987). Silica/iron oxide nanoparticles were flame-generated from iron pentacarbonyl and hexamethyldisiloxane in a premixed methane/oxygen/nitrogen flame (Ehrman et al. 1999). Each particle contains both  $\gamma$ -Fe<sub>2</sub>O<sub>3</sub> and silica. Lastly, the gold particles were produced via sodium citrate reaction with HAuCl<sub>4</sub> in water followed by the addition of polyethylene glycol (PEG) to coat the surface (Graber et al. 1995).

Table 1. Characteristics of the inorganic nanoparticles used in experimentation.

	Mean radius (nm)	Concentration per flask (g/mL)	Crystalline structure	Surface chemistry
Silica	$60 \pm 0.2$	$3.303 \times 10^{-2}$	amorphous	hydrophilic
Silica/Iron Oxide	$80 \pm 0.5$	$2.180 \times 10^{-3}$	crystalline	hydrophilic
PEG-coated Au	$30 \pm 0.2$	$1.130 \times 10^{-4}$	crystalline	hydrophilic

## 2.2 Culture Media and Culture Conditions

For rapid growth of the microbial cells, Luria Bertani (LB) medium was prepared and sterilized for each experiment. 250 mL shake flasks were also sterilized before experimentation. 100 mL of LB medium was transferred to each flask. Various concentrations of nanoparticles were carefully placed into each flask, leaving one as a control to track the normal growth of the microbial cells without nanoparticles.

Each flask was then inoculated with 1 mL of *E. coli* (pBR322 JM105) grown in liquid LB medium. The flasks were shaken at 180 rpm and 37°C in a shaking water bath. Optical density measurements from each flask were taken every thirty minutes to record the growth of the microbes from inoculation through late exponential phase using a spectrophotometer set at 600 nm. The growth rate of microbial cells interacting with the nanoparticles was determined from a plot of the log of the optical density versus time.

### *2.3 Particle Morphology using Transmission Electron Microscopy*

Transmission electron microscopy (TEM) was used to obtain images of the nanoparticles. Silica/iron oxide samples were prepared for TEM imaging by inserting a TEM grid (copper coated with formvar) into dry powder using tweezers to hold the grid. The sample grid was then lightly tapped to remove any excess particles, and the grid was placed in the TEM for imaging. Although in solution, the silica and gold samples were also prepared by inserting the TEM grid into each liquid sample. The sample grids were then allowed to air dry overnight.

### *2.4 Characterization of Nanoparticles by Dynamic Light Scattering*

One of the more common methods employed to characterize pharmaceutical colloids is dynamic light scattering (DLS). Analysis of the size distribution of the nanoparticles was performed using a DLS autocorrelation tool known as Photocor<sup>®</sup>. DLS measurements were taken of the nanoparticles in distilled water and in LB growth media. With this procedure, the difference between the behavior of the nanoparticles in solutions with and without salt was compared.

### *2.5 Nanoparticle/Cell Interaction Studies Using TEM*

After characterizing the various nanoparticles, experiments were conducted to observe the relationship between the iron oxide composite nanoparticles and *E. coli* in LB media. Cell/nanoparticle interactions were observed using a Zeiss EM10 CA transmission

electron microscope at the University of Maryland Biological Ultrastructure Facility. Samples of *E. coli* were withdrawn at points during late exponential phase (optical density  $\sim 0.600$ ). After collection, they were centrifuged and suspended at room temperature in 0.12M Millonig's phosphate buffer at pH 7.3 and later with 2% glutaraldehyde. The cell pellets were then washed again with buffer, and then secondary fixed with 1% OsO<sub>4</sub>. At this point, they were washed with distilled water and then postfixed with 2% uranyl acetate, rinsed in buffer and double distilled water, dehydrated in a series of ethanol and propylene oxide immersions, and embedded in Spurr's resin. A diamond knife was used to section the embedded cells. The sections were post-stained with 2.5% aqueous uranyl acetate and 0.2% aqueous lead citrate.

### **3.0 Results**

#### *3.1 TEM Measurements*

According to the micrographs, the morphology of the silica/iron oxide nanoparticles is approximately spherical. The mole ratio of silica to iron oxide is roughly 1:1, and Figure 1 shows the nanoparticles with the dark side being iron oxide and the lighter side being silica. The average particle size was 80 nm (standard deviation 0.5 nm).

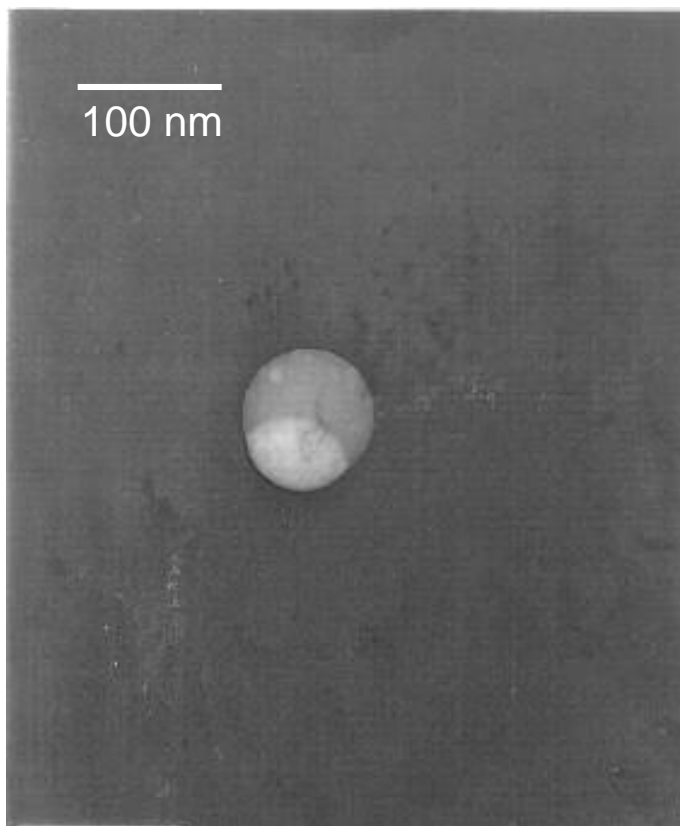


Figure 1. TEM of a  $\text{SiO}_2/\gamma\text{-Fe}_2\text{O}_2$  particle generated in a premixed flame.

Figure 2 is a micrograph of the gold nanoparticles indicating that they are also spherical with an average size of 30 nm (standard deviation 0.2 nm). Lastly, the silica nanoparticles were analyzed using TEM, and the results show spherical morphology with an average particle size of 60 (standard deviation 0.2 nm). Figure 3 is a micrograph of the silica nanoparticles taken in aqueous solution.

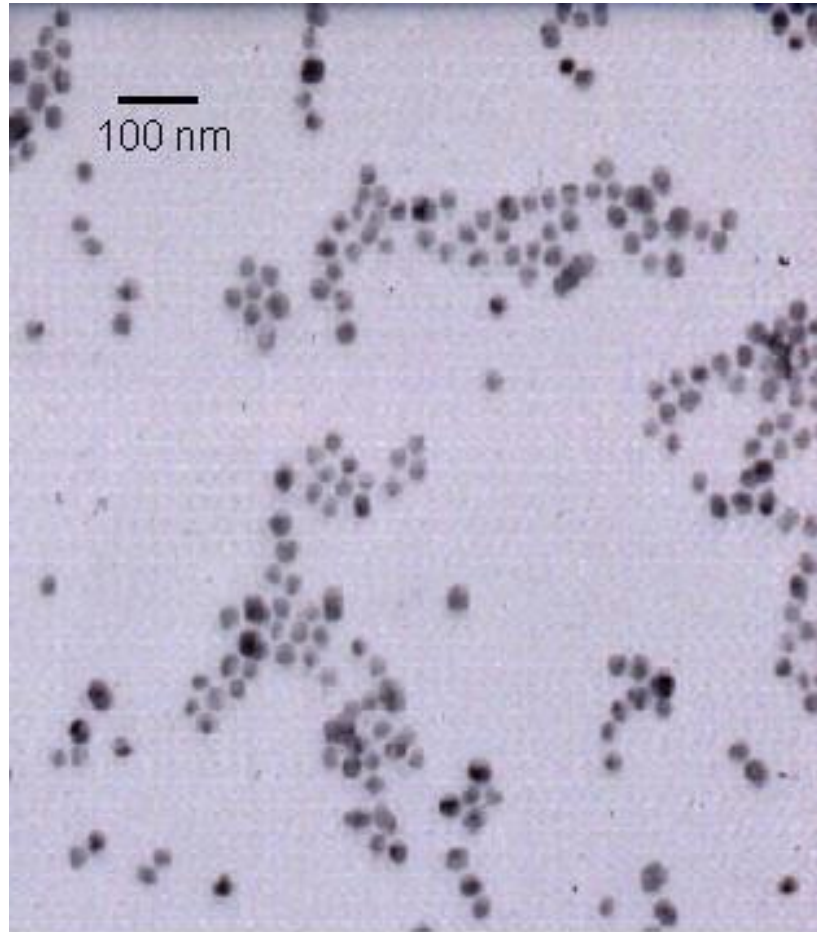


Figure 2. TEM image of gold particles without PEG coating (Majetich).

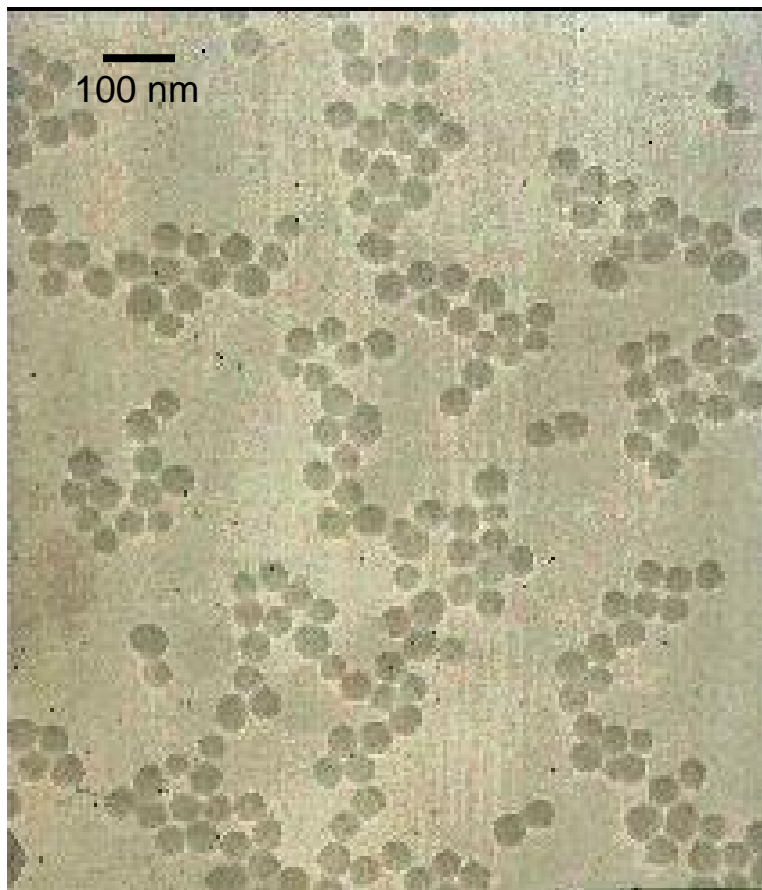


Figure 3. TEM image of silica nanoparticles.

The micrographs of *E. coli*, in the presence of iron oxide composite nanoparticles, indicate that the cells are able to maintain growth, showing no overt signs of toxicity. There appears to be an association of the nanoparticles with the cell membrane, but it is not clear if this is a specific or nonspecific interaction. Figure 4 shows the physical relationship between *E. coli* and composite iron oxide nanoparticles.

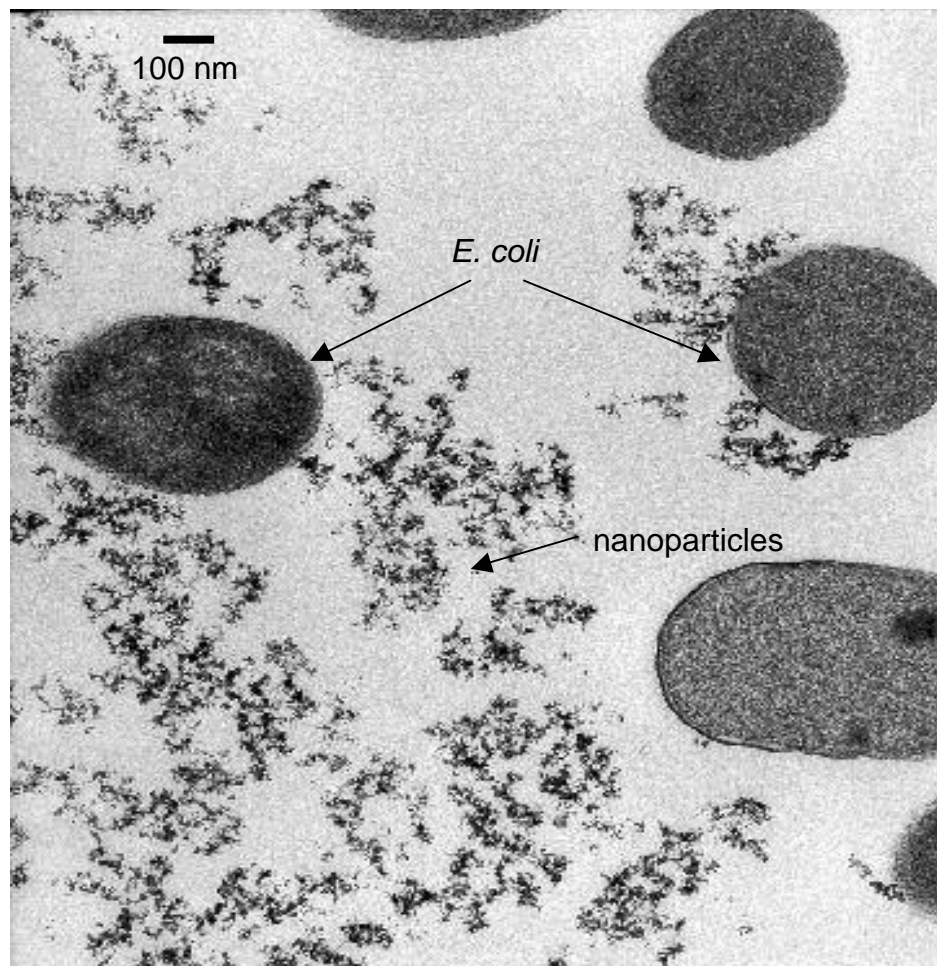


Figure 4. TEM micrograph of cross sections of *E. coli* grown with composite iron oxide nanoparticles.

### 3.2 DLS Measurements

Nanoparticles have a tendency to agglomerate in solution due, in part, to the characteristics of the liquid medium with the addition of salt. In regards to the nanoparticles and microbial cell interactions, this will greatly affect the behavior of the cells. Non-agglomerated particles suspended in solution are preferable for testing purposes because of the following:

- 1) free moving, single unit particles have more contact with microbes.
- 2) translocation through the cell membrane will be accelerated due to size.

LB media contains a high salt concentration (0.2 M) that may contribute to the agglomeration of the nanoparticles. The surface charge on the nanoparticles in solution allows the nanoparticles to attract to one another because of the influence of ions from the salts, therefore resulting in the formation of large agglomerates. As a result, the nanoparticles may fall out of solution and settle to the bottom of the shake flasks.

As time increased, the mean particle radius increased. The agglomerate size for the silica particles ranged between 300-360 nm, as shown in Figure 5. Figure 6 shows DLS measurements for silica/iron oxide, indicating similar behavior in the LB media. In contrast, the PEG-coated gold nanoparticles remained stable in LB media, thus retaining their size without forming large agglomerates.

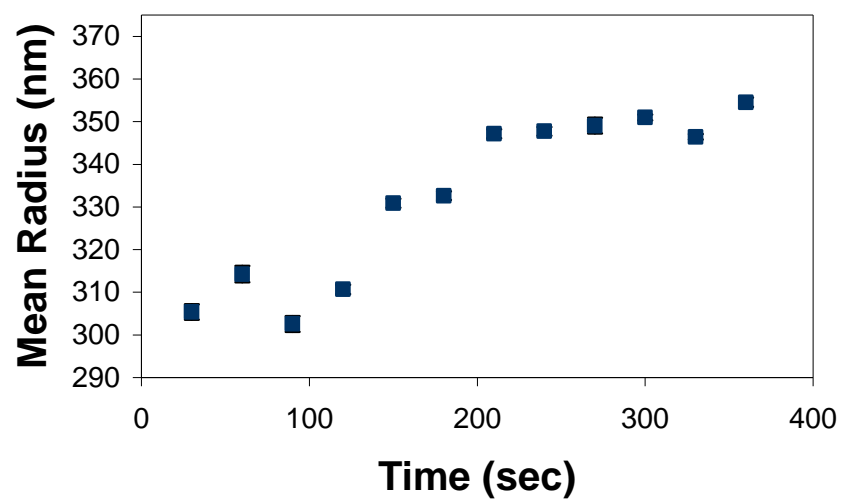


Figure 5. Results of DLS for silica in LB media show that the nanoparticles agglomerate in solution.

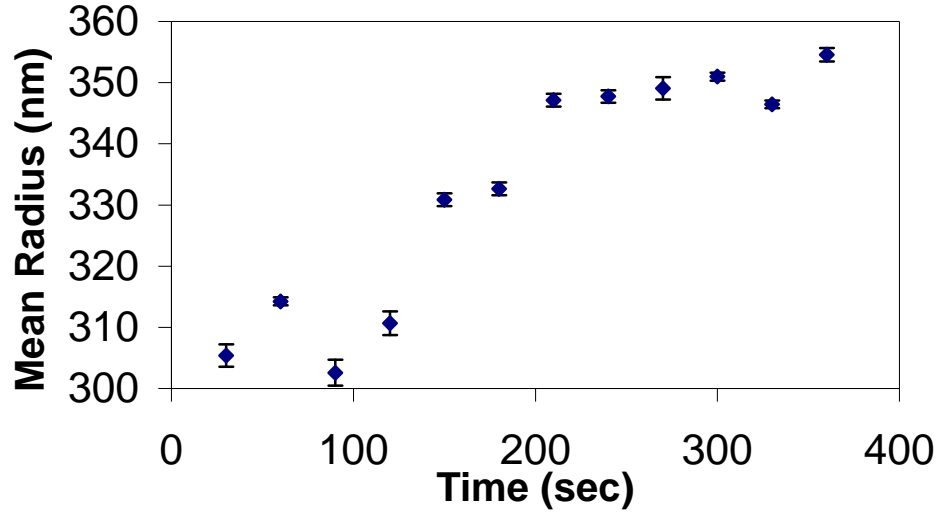


Figure 6. DLS measurement of silica/iron oxide particles in LB media.

### 3.3 Growth Experiments

The overall results indicated that the growth of *E. coli* exposed to silica, silica/iron oxide, and gold nanoparticles was uninhibited. Growth curves were generated for *E. coli* growing with  $2.180 \times 10^{-3}$  g/mL of silica/iron oxide nanoparticle solution. Under these growth conditions, there was no evidence that the nanoparticles prevented the microbial cells from growing. Figure 7 illustrates the growth curves for *E. coli* growing with and without silica/iron oxide nanoparticles. Results indicate that there is little difference between the two curves.

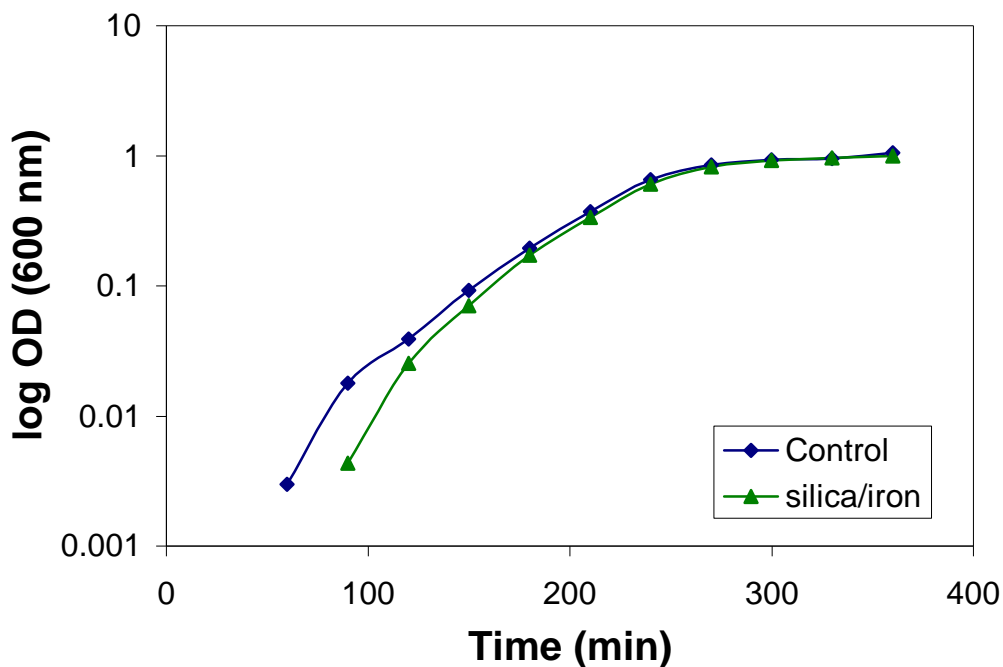


Figure 7. Growth curves of *E. coli* in the presence of silica/iron oxide nanoparticles.

Another experiment was conducted using pure silica nanoparticles at the same volume as the silica/iron oxide experiment. Growth data was taken for  $3.303 \times 10^{-2}$  g/mL of silica solution in 100 mL of LB media. Figure 8 depicts the growth curves for this experiment.

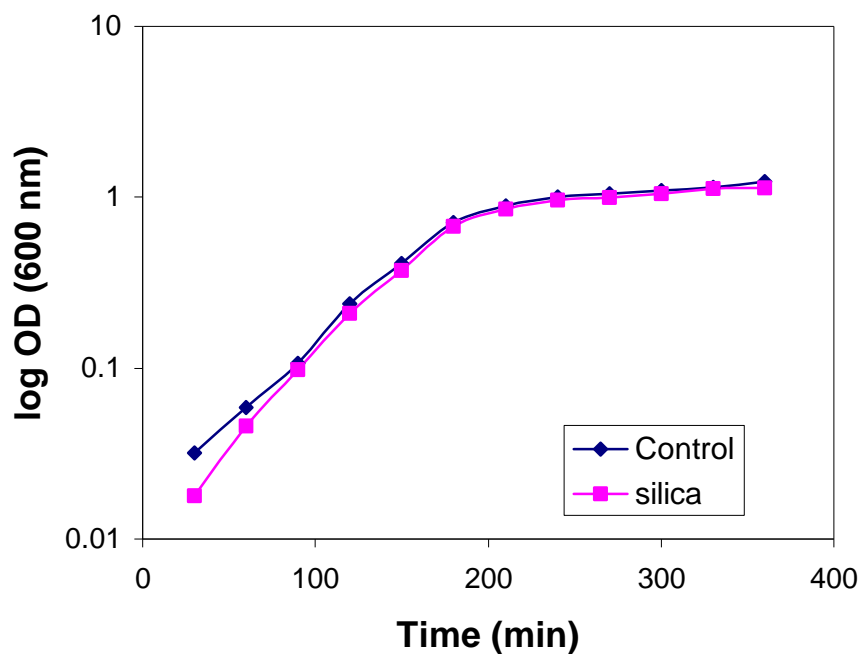


Figure 8. Growth curves for *E. coli* in the presence of silica nanoparticles.

As with the silica and silica/iron oxide experiments, a toxicity study was performed using the gold nanoparticles at a concentration of  $1.130 \times 10^{-4}$  g/mL. The gold particles show greater stability in solution due to the coating of PEG on the surface. This allows the particles to not only stay suspended in solution, but they are able to sustain

their initial radius of 30 nm. Figure 9 indicates that there is little if any affect on growth due to the presence of the gold nanoparticles.

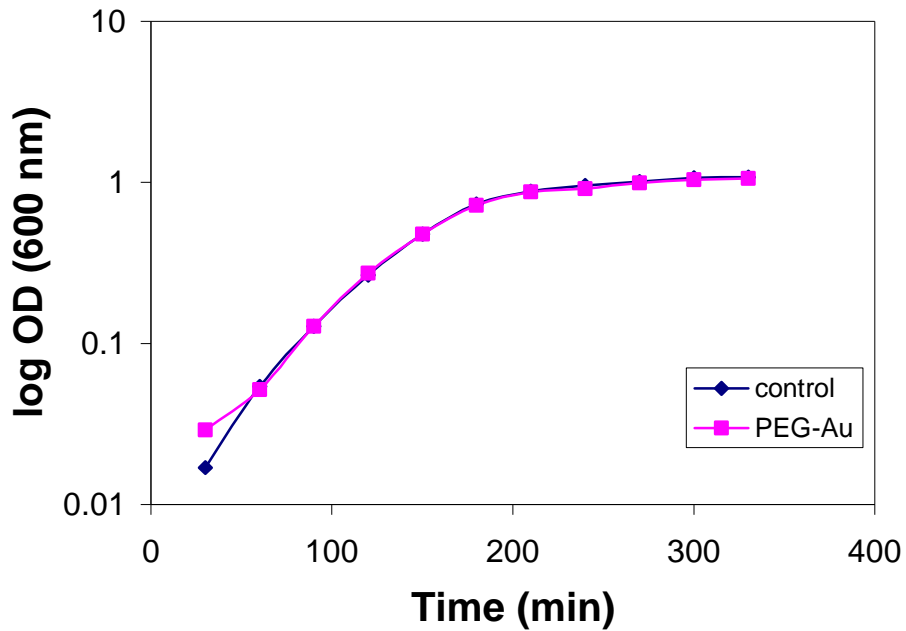


Figure 9. Growth curves of *E. coli* in the presence of PEG coated gold nanoparticles.

A final experiment was conducted to test the influence of the composite iron oxide nanoparticles on *E. coli* at concentrations much higher than the previous experiments. The amount of the composite nanoparticles was increased to  $2.180 \times 10^{-2}$  g/mL in one flask and  $4.36 \times 10^{-2}$  g/mL in a separate flask. Optical density measurements showed that *E. coli* was not inhibited by the increase in nanoparticle concentration (Figure 10).

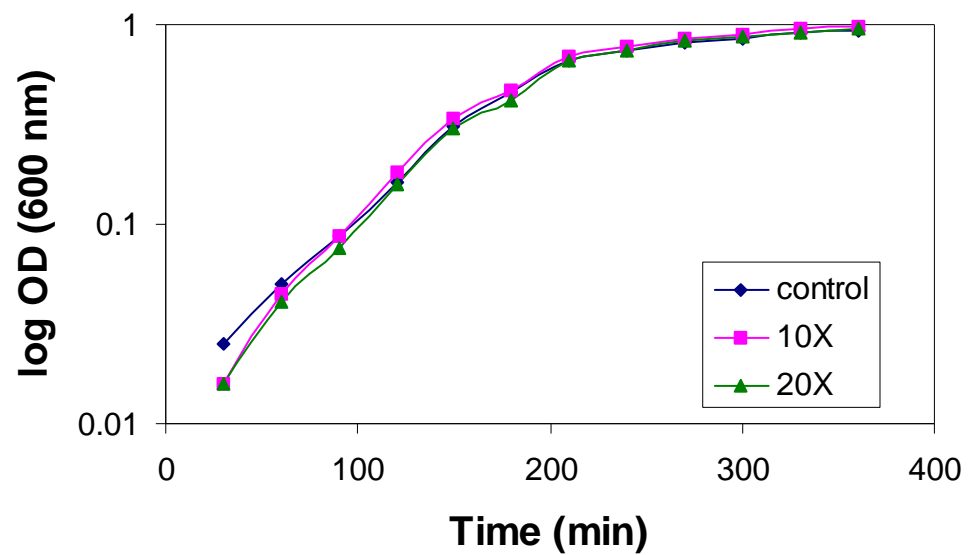


Figure 10. Growth curves of *E. coli* in the presence of higher concentrations of composite iron oxide nanoparticles.

#### **4.0 Conclusion**

Preliminary studies were performed to determine if nanoparticles affect the growth of microbial cells by studying cell cultures in the presence of several inorganic nanoparticles. In addition, understanding the colloidal properties of the inorganic nanoparticles was an important factor to ensure the stability of the nanoparticles in microbial growth media. Methods, such as dynamic light scattering (DLS) and transmission electron microscopy (TEM) were used to quantify size distribution and determine morphology of the nanoparticles, respectively.

Dynamic light scattering results suggests that, with the exception of gold, the nanoparticles were agglomerates in solution. The gold particles used in the experiments were coated with PEG, which proved to be a viable means to promote particle stability. In future studies, experimentation will take place with particles that are less agglomerated and more stable. Various surface chemistry techniques will be used to stabilize the particles in growth media.

Future work will include fluorescently tagging the composite iron oxide nanoparticles and monitoring the binding of the nanoparticles to the membrane surface and/or uptake of the nanoparticles in mammalian cell cultures using fluorescent microscopy. Other means of promoting particle stability in cell culture media will also be explored. Investigating the intracellular and extracellular location of the iron oxide nanoparticles in mammalian cell cultures will answer questions about how the nanoparticles behave and where within the cell they migrate.

## CHAPTER 4– SURFACE MODIFICATION OF MAGNETIC NANOPARTICLES USING GUM ARABIC

### Abstract

Magnetite nanoparticles were synthesized and functionalized by coating the particle surfaces with gum arabic (GA) to improve particle stability in aqueous suspensions. Particle characterization was performed using transmission electron microscopy (TEM) and dynamic light scattering (DLS) to analyze the morphology and quantify the size distribution of the nanoparticles, respectively. The results from DLS indicated that the GA-treated nanoparticles formed smaller agglomerates as compared to the untreated samples over an extended period of time. Thermogravimetric data show that GA has a strong affinity toward the oxide surface with an average weight loss of 23%. Zeta potential measurements indicated that the treated nanoparticles were more negatively charged due to the presence of anionic GA at the surface. GA contributed to steric stabilization which, therefore, prevented the nanoparticles from further agglomeration in aqueous solution. Adsorption studies were performed and determined that GA adsorption onto magnetite follows the Langmuir adsorption isotherm.

### 1. Introduction

Biocompatible, stable magnetic nanoparticles are of interest for applications ranging from magnetic resonance imaging (MRI) to biosensing. Research in the area of synthesizing iron oxide nanoparticles has been underway for many years,

along with the attempt to mitigate the problem of colloid stability for these particle systems. During synthesis, iron oxide nanoparticles tend to agglomerate in order to reduce their surface energy by the strong magnetic dipole-dipole attractions between particles (Kim et al. 2001b). Many methods have been proposed to solve this problem, however not all of the methods yield known biocompatibility.

Several studies in the area of surface modification for iron oxide nanoparticles have focused on using surfactants to control particle size, along with other materials to improve biocompatibility (Prozorov et al. 1999). Dextrin and polyethylene glycol (PEG) are both commonly used polymers for coating materials for biological applications, such as MRI. Tetramethylammonium hydroxide (TMA) is a known agent for redispersing agglomerated iron oxide nanoparticles because it is a low polarizing cation that favors solution stability (Massart 1981). However, TMA is unlikely to be a biocompatible means of coating nanoparticles because it is highly basic. Although the materials mentioned are frequently used in experimentation, few of them act as efficient, long term dispersing agents in aqueous environments.

A natural polymer known as Gum Arabic (GA) has recently shown the ability to sustain colloidal stability for systems of carbon nanotubes in aqueous solutions due to nonspecific physical adsorption (Bandyopadhyaya et al. 2001). It has also been used in the preparation of colloidal silver particles as a steric stabilizer (Velikov et al. 2003). GA is a remarkable and complex material used in various industries as an emulsifier and stabilizer for oils and flavorings (Dickinson 2003; Islam et al. 1997; Ray et al. 1995; Tischer et al. 2002). It is made up of a high

molecular weight glycoprotein and a lower molecular weight polysaccharide. The GA molecule contains a charged group, and when adsorbed on a particle surface, it may give rise to non-DLVO surface forces such as steric, bridging, or charge-patched depending on the pH of the particle solution. To date, it is not well understood how GA interacts in solid-liquid dispersions (Leong et al. 2001b). In this paper, we demonstrate the ability of GA to stabilize magnetite dispersions in aqueous mediums.

## **2. Methods and materials**

### *2.1 Synthesis of Magnetite Nanoparticles with and without Gum Arabic*

#### *2.1.1 Magnetite without Gum Arabic*

All synthesis of magnetite nanoparticles was performed using the Massart method (Massart 1981). 20 mL of a 1M FeCl<sub>3</sub> (Acros) solution in water was combined with a 5 mL solution of 2M FeCl<sub>2</sub>• 4H<sub>2</sub>O (Sigma) in 2M HCl. The chloride solutions were prepared quickly, then added to 250 mL of 0.7 M NH<sub>4</sub>OH (purged initially with N<sub>2</sub> gas for 1 hour before adding salts) in an open vessel stirring at 1800 rpm for 30 minutes under a continuous flow of N<sub>2</sub>. Afterwards, the particles were washed by centrifugation and re-suspended using an ultrasonication. Both dynamic light scattering (DLS) and transmission electron microscopy (TEM) were used for characterization.

### 2.1.2 Magnetite with Gum Arabic

This method was similar to the previous magnetite synthesis procedure, with the exception being the addition of GA to the iron salt mixture. GA was used to study its affect on particle synthesis. 10mL of 10% GA solution was added to the iron salt solution. As before, the two chloride solutions were immediately mixed together (1:2 molar ratio  $\text{FeCl}_3$  to  $\text{FeCl}_2$ ) and poured into an open vessel containing the base solution which was purged continuously with  $\text{N}_2$  gas. The chloride solutions were made immediately before each experiment to avoid  $\text{Fe}^{3+}$  from becoming goethite ( $\text{FeO}(\text{OH})$ ) and to keep  $\text{Fe}^{2+}$  from oxidizing in air (Phillipse et al. 1994). The chlorides and base solution were vigorously mixed at 1800 rpm in a mechanical stirrer. The solution instantly turned black in color, similar to that reported in literature. Mixing occurred for 30 minutes.

### 2.2 Surface modification using Gum Arabic

As mentioned previously, GA has the ability to stabilize emulsions quite effectively. However, its potential use as a stabilizer of solid liquid interfaces is not well understood. GA was used in this work as a coating material to help alleviate the problem of further agglomeration in biological mediums. Biological mediums have relatively high salt concentrations that, in part, may give rise to flocculation of particles, particularly in the nanometer regime. Given that iron oxide nanoparticles agglomerate during synthesis, additional agglomeration might be considered less desirable for certain biological applications, such as targeted

drug delivery. A protective, charged coating that responds in a non-DLVO fashion is ideal for this situation to minimize reduction of the electric double layer.

GA was used as a coating material for both magnetite precipitated with and without GA. A 25 mL sample of magnetite was centrifuged to remove the supernatant and resuspended in deionized water. 100 mg of GA was added to the sample and mildly sonicated to disperse the GA material. This method allowed the GA to mix thoroughly in the sample. After sonication, the sample was washed several times to remove any excess GA. The coated samples were then tested with M9 minimal media to observe their behavior using DLS over time. Uncoated magnetite was used as the control for comparison.

### *2.3 Characterization of GA-coated and GA co-precipitated magnetite nanoparticles*

#### *2.3.1 Particle morphology using transmission electron microscopy (TEM)*

Samples were prepared for TEM imaging by inserting TEM grids (copper coated with formvar) into diluted liquid samples. The liquid samples consisted of washed particles suspended in deionized water. Several samples were washed and diluted in ethyl alcohol to remove excess organic material to improve dispersion of particles, as well as to improve microscope imaging. The samples were observed using a Hitachi 600AB transmission electron microscope.

#### *2.3.2 X-ray diffraction (XRD)*

The powder X-ray diffraction analysis was conducted on a Bruker D8 X-ray diffractometer at a scanning rate of 4 degrees per minute with  $2\theta$  ranging from  $5^\circ$  to

100°, using Cu K $\alpha$  radiation ( $\lambda = 1.5418 \text{ \AA}$ ). The untreated samples were tested to verify the formation of magnetite nanoparticles.

### 2.3.3 Size distribution using dynamic light scattering (DLS)

One of the more common methods employed to characterize colloidal systems is dynamic light scattering. Analysis of the size distribution of the nanoparticles can be performed using a DLS autocorrelation tool known as Photocor<sup>®</sup>. As with many particles in the nanometer regime, the issue of colloid stability plays a role with the introduction of salt. Nanoparticles tend to agglomerate in saline environments due to the reduction of the protective surface charge known as the electric double layer that surrounds the surface. With DLS, agglomeration can be observed for uncoated magnetite nanoparticles and compared to the coated nanoparticles to test colloid stability in deionized water and M9 microbial growth media.

### 2.3.3 Thermogravimetric Analysis (TGA) analysis

TGA registers the loss or gain in weight of a heated substance as a function of the temperature of the furnace in which it is situated. This method of analysis is useful in determining how much of an organic substance is adsorbed to a particular inorganic species. In this case, the weight of untreated particles is compared to the change in weight of particles coated with GA. The difference between the two is the amount of coating adsorbed on the surface of the magnetite nanoparticles. TGA was performed on each of the 4 samples using a Schimadzu TGA-50

Thermogravimetric Analyzer (Kyoto, Japan). The particles were washed with de-ionized water and dried overnight, yielding an average of 25-30 mg of each sample. The dry solids were then ground into powder using a mortar and pestle. Each sample was weighed in an alumina pan and heated to 1000 °C at a rate of 10 °C/min in air.

#### 2.3.4 FTIR measurements

FTIR spectra are generated for both untreated and treated magnetite nanoparticles, as well as those particles precipitated with GA to help identify the differences between functional groups of the various samples. Samples were prepared as crushed powder weighing approximately 50mg and mixed together with 450mg of crushed KBr. Spectra were taken between 4000 and 800  $\text{cm}^{-1}$ .

#### 2.3.5 BET analysis

The specific surface area was determined using a Nova 1200 Quantachrome. Each sample was weighed initially before degassing at 150°C for 1 hr. After degassing, the surface area was determined by adsorption of  $\text{N}_2$  gas on the magnetic nanoparticles.

#### 2.3.6 Zeta potential measurements as a function of pH.

Zeta potential measurements were taken for both treated and untreated magnetite samples using a Malvern 3000 Zeta-sizer. Particle concentrations were 0.005 wt % in 0.005 M  $\text{KNO}_3$ . The samples were equilibrated over night and then

sonicated before measuring the equilibrium pH and zeta potential. Before each measurement, the sample chamber was flushed out with deionized water to remove any residual sample.

#### 2.3.7. Adsorption studies

Adsorption experiments were conducted with varying concentrations of GA ranging from 1 wt% to 15 wt%. About 0.010g of dried, solid powder in 5 ml of polymer solution were lightly sonicated and set to reach equilibrium in a gyratory shaker for 24 hr. After reaching equilibrium, the samples were centrifuged and washed several times. The supernatant was removed, leaving solid at the bottom that was then dried for TGA analysis. The TGA data was used to construct the adsorption curve depicted in Figure 7.

### 3. Results

TEM images were taken of magnetite particles precipitated with and without GA. As with most magnetite nanoparticles during synthesis, systems of agglomerated nanoparticles were formed in both cases. A major physical difference is seen, however, with those particles synthesized under GA conditions. The GA co-precipitated particles showed more agglomeration compared to those synthesized under the regular Massart method. In both cases, the average primary particle size was between 5 and 10 nm, similar to those reported in literature.

Figure 1a is a micrograph of magnetite precipitated without GA, and Figure 1b depicts magnetite precipitated with GA.

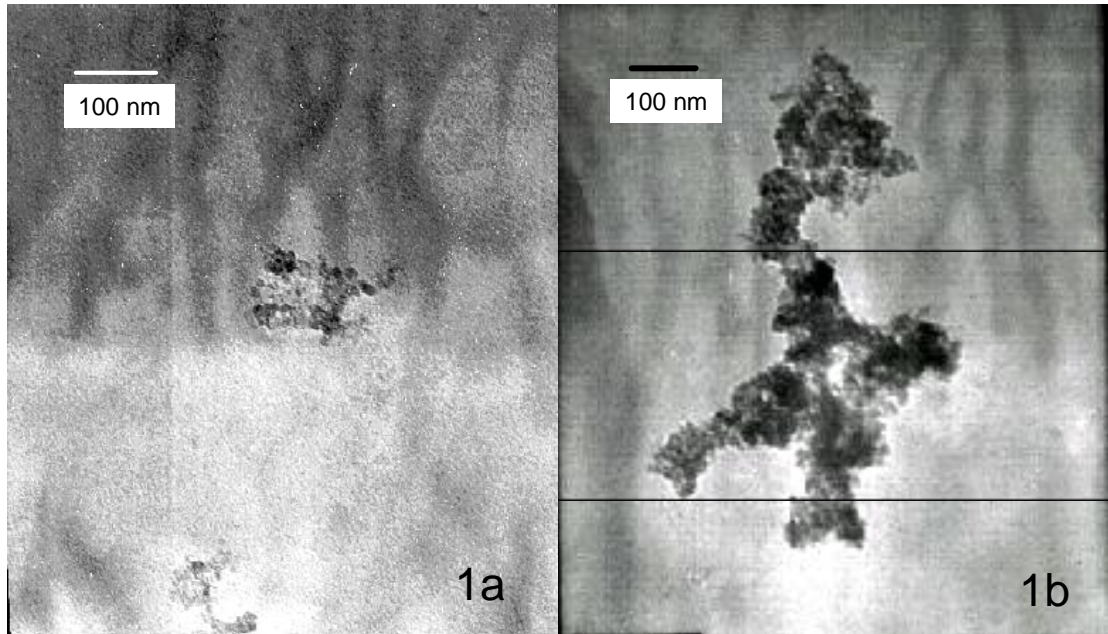


Figure 1a. TEM of untreated magnetite nanoparticles synthesized using the Massart method. Figure 1b. Magnetite nanoparticles co-precipitated with gum arabic. Evidence is seen of larger agglomerates compared to untreated particles.

DLS measurements indicated that GA had the ability to stabilize the magnetite nanoparticles in aqueous media. Even after synthesis, the co-precipitated particles remained suspended in the base solution after several months compared to the untreated particles, which settled out after several hours. Samples were prepared in both deionized water and M9 growth media. Initial readings were taken every minute over a period of ten minutes to track the behavior of the nanoparticles. In

order to get a better idea about how the particles behave over a longer period of time, DLS was conducted over a 30 hour period in deionized water, with readings taken on an hourly basis. Figures 2 and 3 illustrates that there is little change in the hydrodynamic radius for the GA-coated nanoparticles in aqueous solution.

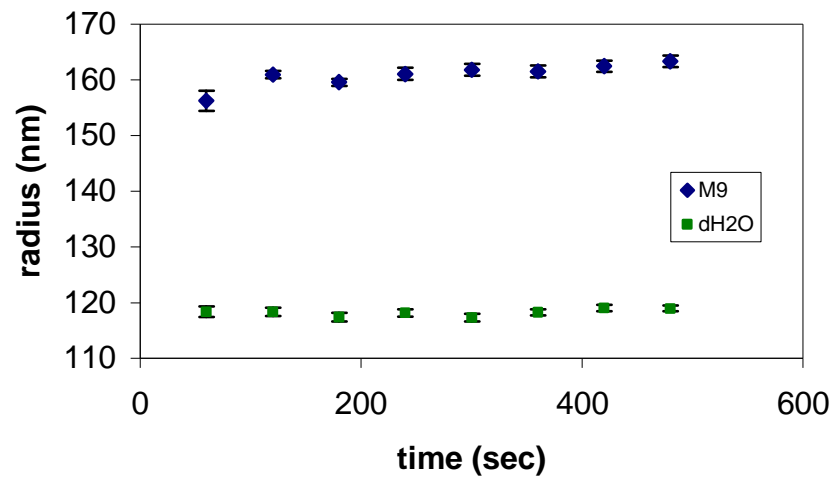


Figure 2. DLS results of GA-coated magnetite nanoparticles in deionized water and M9 minimal media. Small changes occur in the hydrodynamic radius of the samples in M9 media that might be attributed to associated ions in the media.

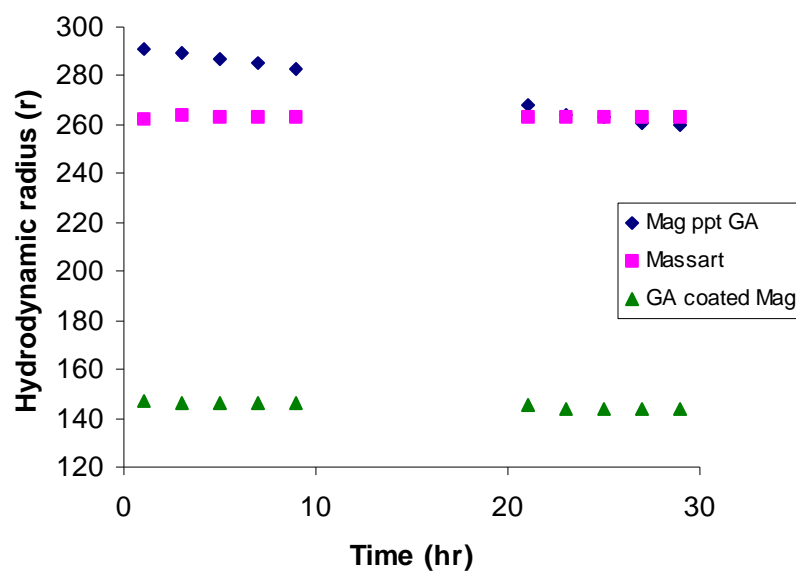


Figure 3. DLS measurements in deionized water of untreated, coated, and co-precipitated samples taken over a 30 hour period. Measurements were recorded for a 9hr period on day 1, left over night, and recorded again for an additional 6hrs.

According to the first set of TGA results (Figure 4), samples of bare magnetite that were coated with GA indicated a total weight loss of 23%. Samples co-precipitated with GA showed a difference in weight loss of 31% due the presence of GA throughout the agglomerates. A second set of TGA results (Figure 5) indicated that there is a maximum concentration of GA that will adsorb to the surface of the magnetite nanoparticles. The adsorption isotherm (Figure 6) illustrates that the surface excess peaks at 0.20 (gram adsorbate per gram of adsorbent) and that it is Langmuir, independent of molecular weight of GA.

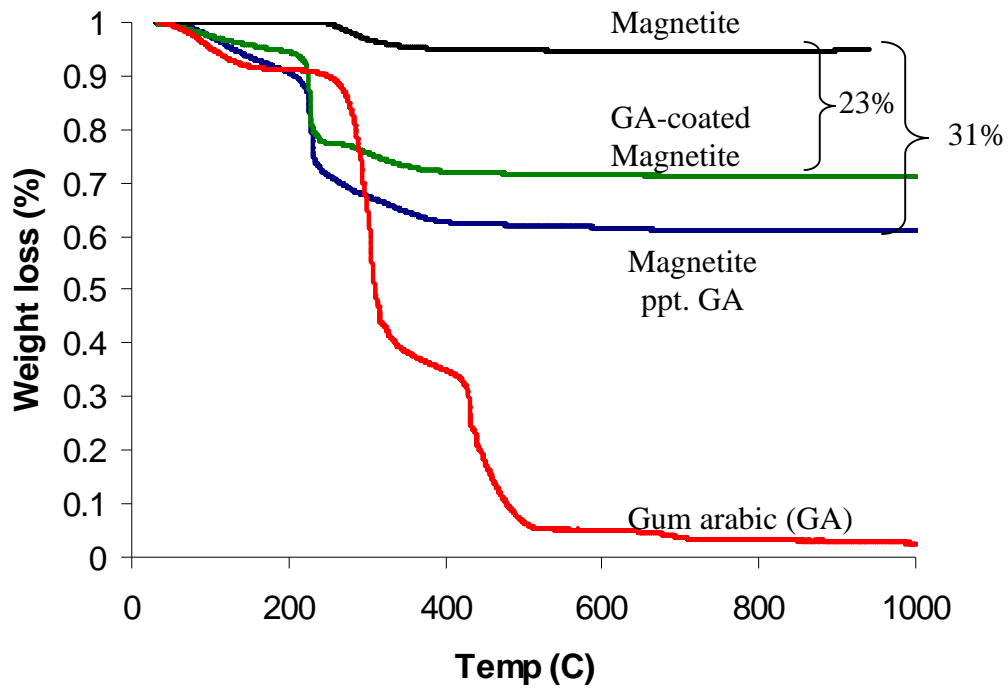


Figure 4. TGA results for untreated nanoparticles, co-precipitated nanoparticles, coated nanoparticles, and gum arabic powder. These results correlate well with the TEM micrographs (Figure 1a and 1b) that compare plain magnetite nanoparticles with GA precipitated magnetite nanoparticles (larger agglomerates due to bridging of GA throughout multiple nanoparticles).

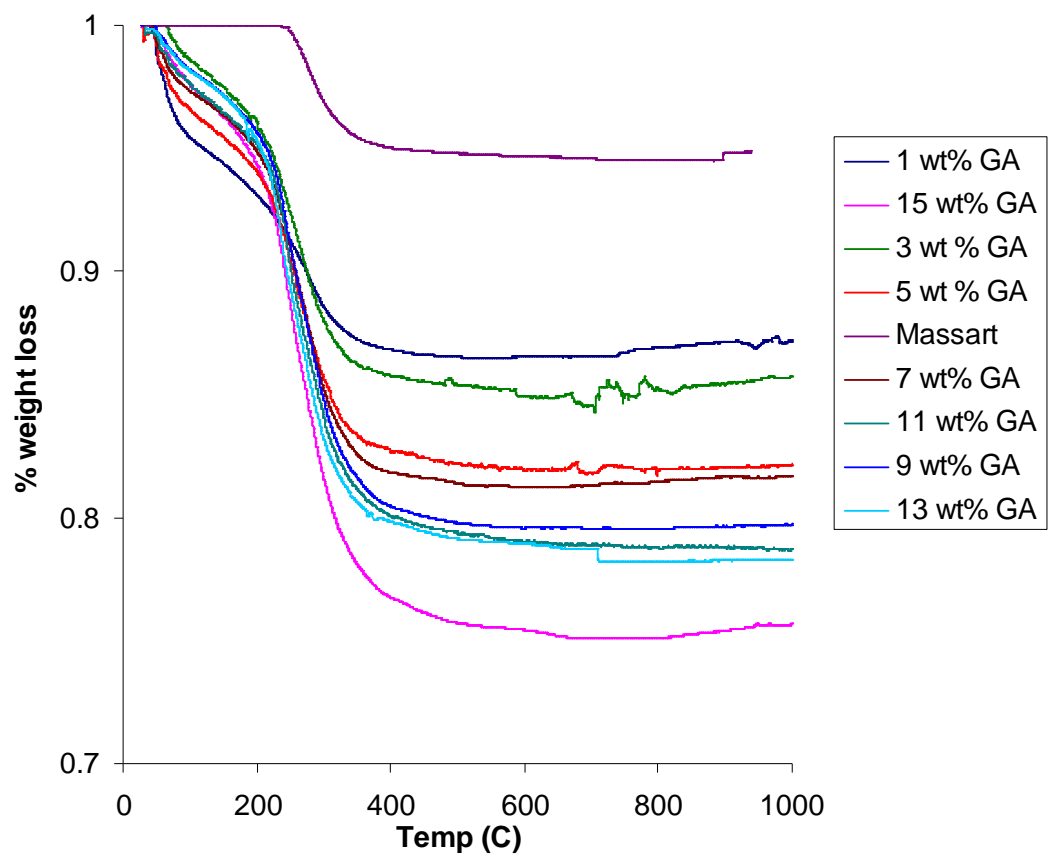


Figure 5. TGA results from concentrations of GA ranging from 1 to 15 wt%. Each sample contained 0.01g magnetite nanoparticles in 5 ml of GA solution.

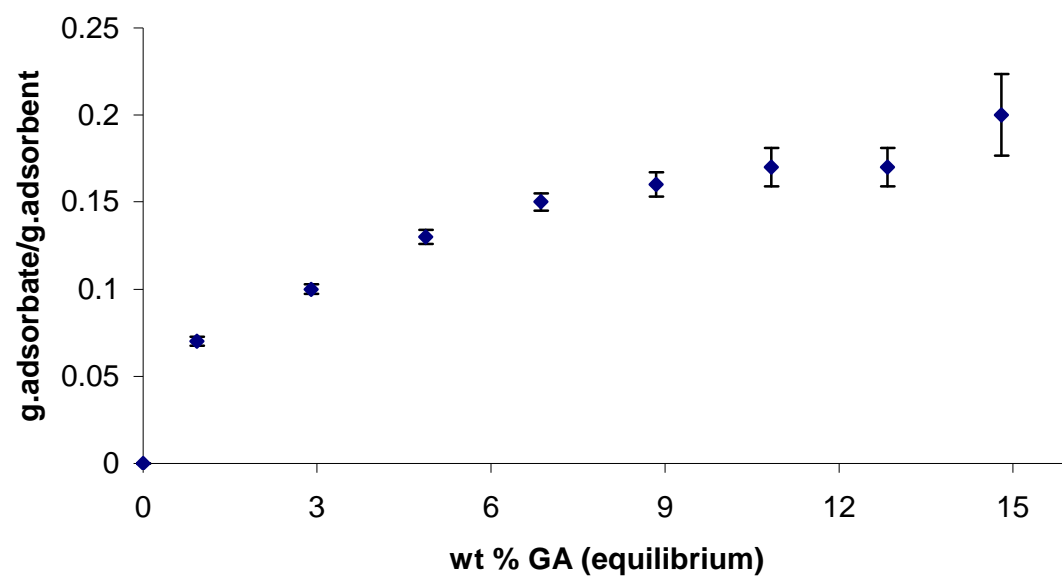


Figure 6. Adsorption isotherm of GA with magnetite nanoparticles extracted from TGA data.

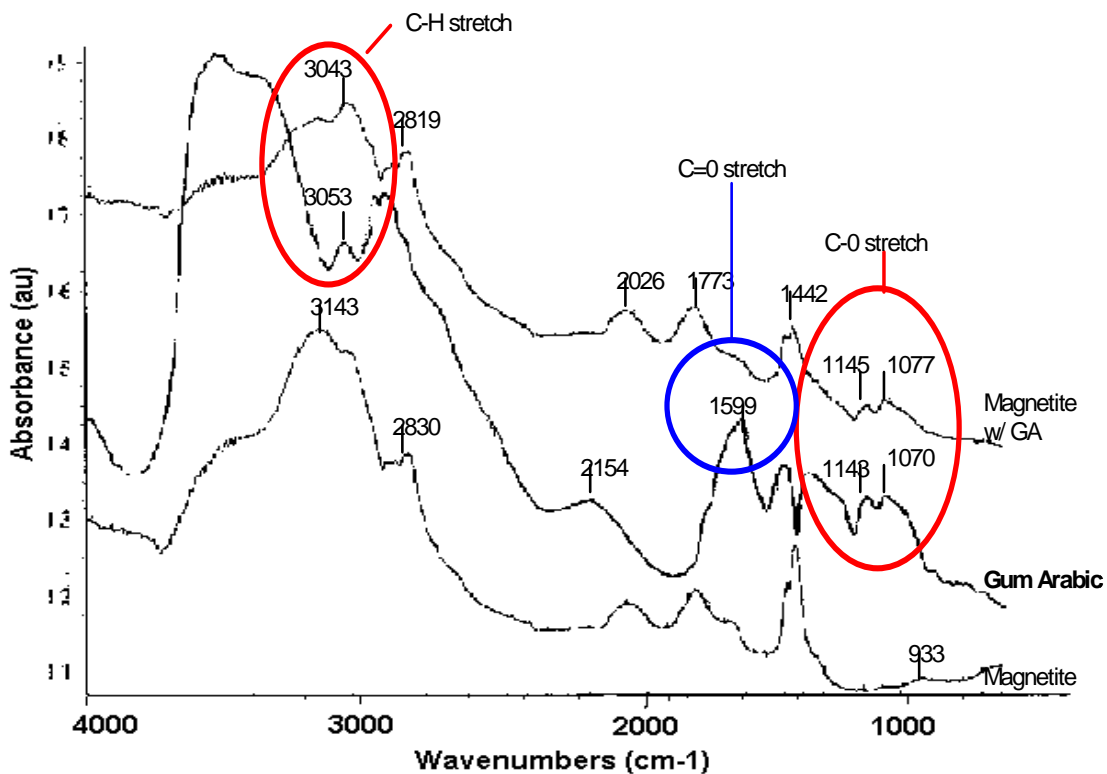


Figure 7. FTIR spectra for untreated magnetite, magnetite coated with gum arabic, and plain gum arabic powder.

From FTIR, it can be seen that, compared to the untreated samples, the treated magnetite particles possess absorption bands at 3043 cm<sup>-1</sup> due to stretching vibrations of the C-H bond, and bands in the regions of 1145 and 1077 cm<sup>-1</sup> due to the C-O bond stretch. A carboxylate group associated with the gum arabic molecule shows a strong peak at 1599 cm<sup>-1</sup> (Figure 7). Figure 10 is a possible reaction mechanism describing the interaction between gum arabic and the iron oxide surface.

BET was used to measure the specific surface area for the untreated magnetite samples. The untreated samples had a measured specific surface area equal to 200 m<sup>2</sup>/g. This results in a diameter of approximately 6 nm per primary particle that

correlates well with the results from TEM. The XRD measurements taken to verify the formation of magnetite nanoparticles indicate peaks for  $2\theta$  at locations similar to those reported in literature (Figure 8).

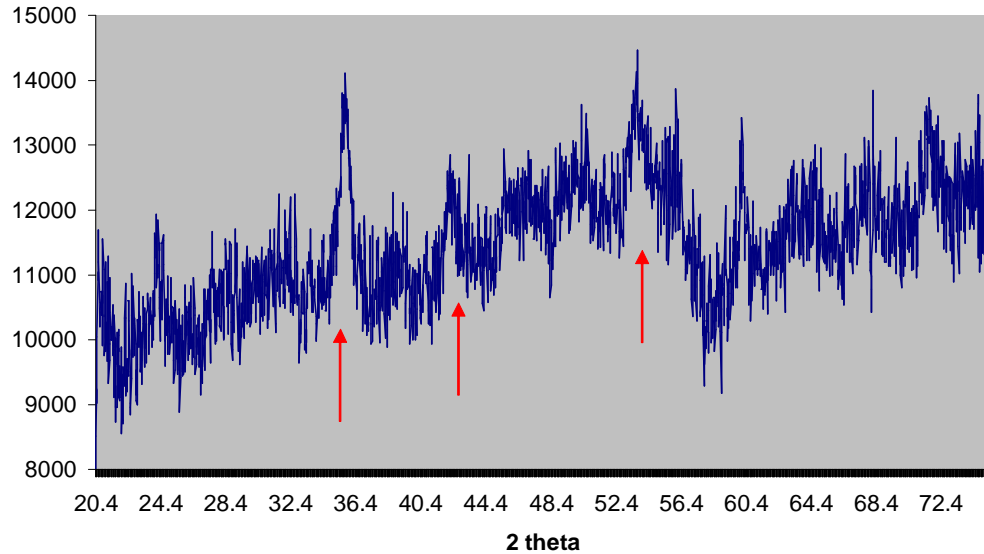


Figure 8. X-ray diffraction pattern for magnetite nanoparticles.

The zeta potentials of treated and untreated magnetite samples as a function of pH are presented in Figure 9. The curve for the untreated samples crossed at a value of pH 4.2 for the point of zero charge ( $\text{pH}_{\text{PZC}}$ ). For the treated samples, the  $\text{pH}_{\text{PZC}}$  equaled 3.8. The overall values for the zeta potentials for both samples fell between 10 and -30 mV.

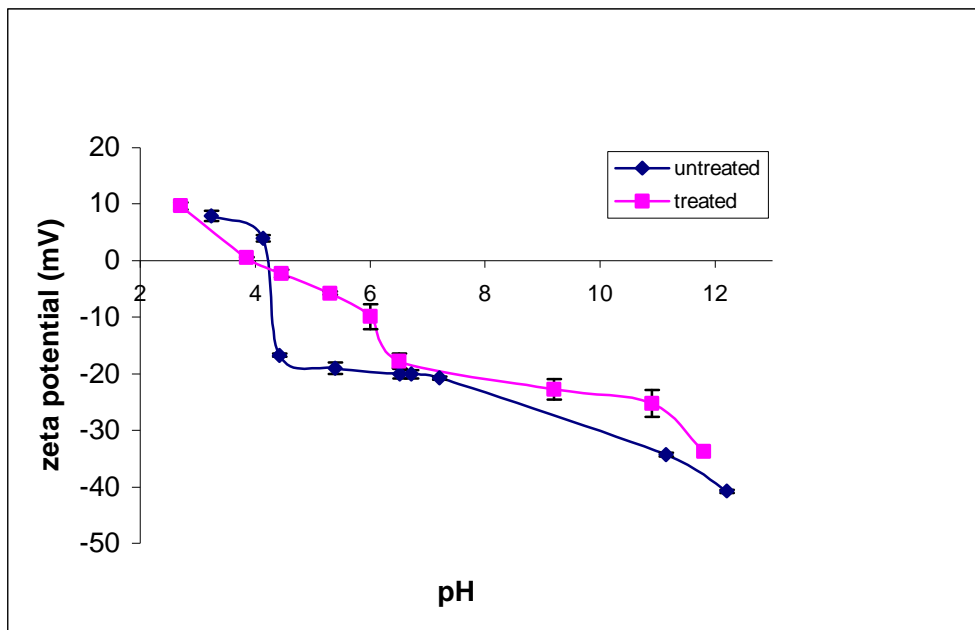


Figure 9. Zeta potential measurements comparing GA-coated magnetic nanoparticles with untreated nanoparticles. GA (anionic) causes a shift to the left, indicating a more negative surface charge.

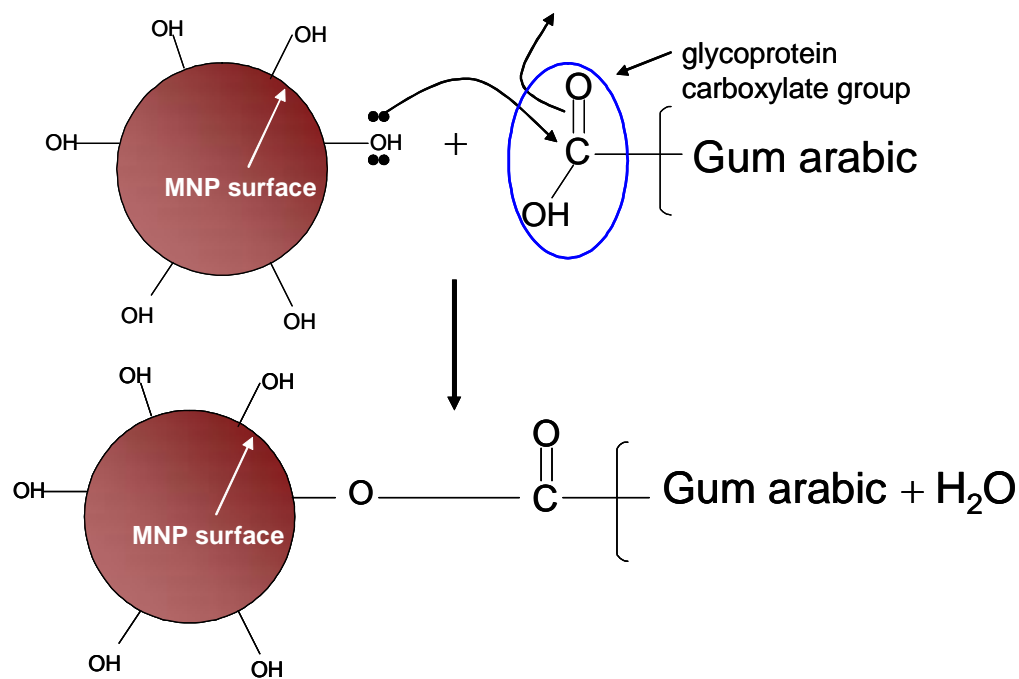


Figure 10. A possible reaction mechanism for the attachment of the gum arabic molecule to the iron oxide surface.

#### 4.0 Discussion

It is apparent from these results that there is a strong physical adsorption of GA onto the surface of the magnetite nanoparticles. It has been postulated that the glycoprotein in GA is capable of strong binding interactions due to the electrostatic attraction between a negatively charged group of a GA molecule and a positive site on the oxide surface (Leong et al. 2001b). During co-precipitation, a bridge may form when part of the glycoprotein is adsorbed onto the surface of two or more particles. This may explain why the co-precipitated particles form larger agglomerates and show more weight loss compared to the untreated samples.

In the FTIR spectra, the lower frequencies are indicative of strong hydrogen bonds that are attributes of carboxyl groups (Coates J. 2000). An adsorbed GA glycoprotein molecule contains both adsorbed and free carboxylate and amino groups. The free carboxylate groups attach to the particle surface when the negatively charged group of GA binds to a positive site on the surface of the iron oxide (Leong et al. 2001b). Spectra were taken of plain GA showing bands in similar positions as the treated samples, illustrating that GA was present on the treated samples.

Zeta potential measurements provide further confirmation that GA contributes to steric stabilization of the nanoparticles in aqueous solution. Because the values for treated and untreated samples fall between 10 mV and -30 mV, this indicates that the nanoparticles are unstable dispersions. However, GA is more negatively charged than the plain oxide surface illustrated by a leftward shift of the curve. The hydrophilic, polysaccharide molecules of GA repel each other, preventing further agglomeration of the nanoparticles in solution.

## **5.0 Conclusion**

Gum arabic is a surface-active molecule capable of improving magnetic nanoparticle stability in aqueous solutions by providing steric stabilization. The natural polymer has a strong affinity for the oxide surface due to the binding of the carboxylate groups to sites along the oxide surfaces. It was also determined that GA adsorption onto the surface of magnetite nanoparticles is independent of molecular weight.

Future studies will focus on determining how GA affects particle synthesis by varying its concentration in either base solution or iron salt solution. The order in which it is added might impact how the nanoparticles are formed (i.e. size, crystallinity, agglomeration, etc.). Other studies will involve using GA-modified nanoparticles for investigating interactions with various cell types. It is possible that GA may serve as a new material for not only increasing particle stability, but also as a means for promoting nanoparticle/cell interactions.

## **CHAPTER 5 – GUM ARABIC MODIFIED MAGNETIC NANOPARTICLES: INFLUENCE ON PROSTATE CARCINOMA CELLS IN VITRO**

### **Abstract**

Various polymers have been used to increase the biocompatibility and overall stability of magnetic nanoparticles for medical and other biological applications, but awareness has been drawn to the importance of developing and discovering new materials that can promote interactions between nanoparticles and cells. In this study, gum arabic was used to modify magnetic nanoparticles. It was determined that gum arabic facilitates the internalization of magnetic nanoparticles in prostate carcinoma cell line DU145 as seen by immunofluorescent images of particles coated with FITC-labeled gum arabic. Transmission electron microscopy revealed concentrations of the treated particles in the secondary lysosomes and vacuoles of the Golgi zone in the cancer cells. DAPI stained cells differentiated between healthy nuclei and nanoparticle-loaded cytoplasm, which correlated well with TEM. Untreated particles showed insignificant internalization in the cells.

### **1. Introduction**

Interactions between surface-modified magnetic nanoparticles and mammalian cells have been under serious investigation for many years. Issues dealing with targeted biodistribution of these nanoparticles results from concerns involving ways to prevent nanoparticles from becoming unstable in a physiological environment (i.e. bloodstream), thus potentially leading to a quick and efficient process known as opsonization (Berry and Curtis 2003). In this event, rapid clearance of the nanoparticles occurs due to plasma

components that bind to the surface and make them recognizable by the reticulo-endothelial system (RES), a specialized system that removes them from circulation (Babes et al. 1999; Berry et al. 2004; Gaur et al. 2000a; Moghimi et al. 2001; Moore et al. 2000; Wilhelm et al. 2003; Zhang et al. 2001). This occurs when particles with large amounts of hydrophobic surface area are introduced into the system because they are efficiently coated with plasma proteins. In contrast, hydrophilic surfaces resist opsonization and are more likely to remain in circulation (Berry et al. 2003).

Various types of coating materials have been explored to increase the stability and biocompatibility of magnetic nanoparticles. In literature, the most common coatings are derivatives of dextran, polyethylene glycol (PEG), polyethylene oxide (PEO), poloxomers, and polyoxamines (Moghimi et al. 2001). Out of the coatings listed, dextran is widely used for coating particles for MRI contrast agents and other biological applications. However, there have been reports of cellular uptake of dextran-modified nanoparticles that resulted in cell damage and reduced cell proliferation (Berry et al. 2003; Jordan et al. 1999). From examples such as this, it has become more evident that there is a need to explore other sources of coating materials for improving nanoparticle biocompatibility and stability.

Focusing primarily on cancer cells, these cells have the ability to sense complex sugars that allow them to bind to other healthy tissue and metastasize. Methods for tagging cancer cells are being developed where modified sugars that contain chemical tags serve as homing devices for both diagnostic and therapeutic applications (Alper 2003). Cancer cells also have a high metabolism and a need for a high energy food source (i.e. complex sugars). In response to this phenomenon, scientists have developed

a cancer fighting technique that involves using iron nanoparticles coated with glucose. The coated particles are injected into a malignant tumor that aggressively metabolizes the particles masked as sugar molecules. It was observed that healthy cells had little interest in the glucose treated particles (James 2003). Once the nanoparticles were engulfed, magnetic fluid hyperthermia was used to destroy the tumor.

In this paper, we demonstrate the uptake of magnetic nanoparticles coated with gum arabic (GA). GA is a remarkable and complex material used in various industries as an emulsifier and stabilizer for oils and flavorings (Dickinson 2003; Islam et al. 1997; Ray et al. 1995; Tischer et al. 2002). It is made up of a high molecular weight glycoprotein and a lower molecular weight polysaccharide. The GA molecule is negatively charged, and when adsorbed on a particle surface, it may give rise to non-DLVO surface forces such as steric, bridging, or charge-patched depending on the pH of the particle solution. To date, it is not well understood what role GA plays in solid-liquid dispersions (Leong et al. 2001a). Our studies using dynamic light scattering showed that GA was an excellent treatment for stabilizing magnetite nanoparticles in biological media. GA is highly biocompatible and because of its complex structure, it is more attractive than simple glucose as a food source due to the combination of sugars and protein in its structural makeup.

## **2. Materials and methods**

### *2.1 Nanoparticle synthesis*

Magnetite nanoparticles were precipitated in alkali media from solutions of Fe (II) and Fe (III) chloride following a technique outlined by Massart (Massart 1981). Particle size was determined by transmission electron microscopy and BET analysis. From these characterization methods, it was determined that the primary particle size was 6 nm. After synthesis, the nanoparticles were washed with deionized water and coated with a 10 wt% gum arabic (Tic Gums, Inc.) solution. The coated particles were centrifuged and washed several times, then re-suspended in deionized water.

### *2.2 Cell Culture*

Cancer cell line DU-145 (BCRC no.60348) was provided from Culture Collection and Research Center, Food Industry Research and Development Institute, Taiwan, Republic of China. DU-145 cells were cultured in Dulbecco's Modified Eagles Medium (DMEM) medium (Sigma) plus 10% fetal bovine serum (FBS) (Hyclone), 0.1 mM non-essential amino acids, 1.0 mM sodium pyruvate, and penicillin/streptomycin (Biochrom AG) at 37°C in a humidified atmosphere at 5% CO<sub>2</sub>. Cell density was 1x 10<sup>6</sup> cells per ml of complete media. The cells were incubated for 24 hrs. At this time point, the cells were incubated in complete medium supplemented with 0.01 mg ml<sup>-1</sup> gum arabic (GA) modified and untreated nanoparticles for an additional 24 hrs. Controls were cultured in the absence of particles.

### *2.3 Localization of FITC-labeled nanoparticles using immunofluorescence*

DU-145 cells, grown on an 8 well glass slide (Lab-Tek II Chamber Slide™ System), were inoculated with FITC (Sigma)-labeled gum arabic nanoparticles (see Appendix A) for 24 hrs (Haugland 2002). They were then fixed with 4 mol % paraformaldehyde for 2 hrs at room temperature and permeabilized with ice-cold methanol for 1 minute. The cells were washed with phosphate buffer saline (PBS) and incubated for 30 minutes to an hour with 1 vol% bovine serum albumin in PBS at room temperature. The specimens were washed with PBS three times and treated with Vectashield mounting medium (Vector Laboratories, Inc. Burlingame, California) covered with cover slips and analyzed using a Zeiss fluorescence microscope.

### *2.4 Cell Viability Assay*

DU-145 cells, grown on 8 well glass slides, were inoculated with TRITC (Sigma)-labeled magnetic nanoparticles coated with gum arabic for 30 minutes (see Appendix B). The cultured cells were washed once with PBS, and then resuspended in PBS containing 0.1 vol % Triton X and incubated for 10 min on ice. The cells were spun down and resuspend in 4 vol % PBS buffered paraformaldehyde solution containing 10 µg/ml 4'-diamidino-2-phenylindole (DAPI, Sigma). 10 µl of the suspension was placed on a glass slide and covered with a coverslip. Once again, the controls were cultured in the absence of nanoparticles.

### *2.5 Nanoparticle/Cell Interaction Studies Using TEM*

Experiments were conducted to observe the difference in nanoparticle uptake between the untreated and treated iron oxide nanoparticles with the cancer cells. Cell/nanoparticle interactions were observed using a Zeiss EM10 CA transmission electron microscope at the University of Maryland Biological Ultrastructure Facility. Samples of DU-145 cells were pre-fixed after incubation using a 4:1 molar ratio of formaldehyde to glutaraldehyde solution. They were then scraped, centrifuged and resuspended at room temperature in 0.12M Millonig's phosphate buffer at pH 7.3. The cell pellets were then washed again with buffer, and then secondarily fixed with 1 vol % OsO<sub>4</sub>. At this point, they were washed with distilled water and then postfixed with 2 vol % uranyl acetate, rinsed in buffer and double distilled water, dehydrated in a series of ethanol and propylene oxide immersions, and embedded in Spurr's resin. A diamond knife was used to section the embedded cells. The sections were post-stained with 2.5 vol % aqueous uranyl acetate and 0.2 vol % aqueous lead citrate.

### 3. 0 Results

Experimental evidence indicated that the untreated nanoparticles were not efficient in undergoing incorporation into the cellular matrix of the prostate carcinoma cells. According to TEM images, the untreated nanoparticles were near the membrane surface, but there was no visible sign of penetration into the cellular membrane (Figure 1). On the other hand, the gum arabic treated nanoparticles were visible not only in the membrane, but also within the Golgi zones (vacuoles and lysosomal regions) of the cultured cells (Figure 2a, 2b).

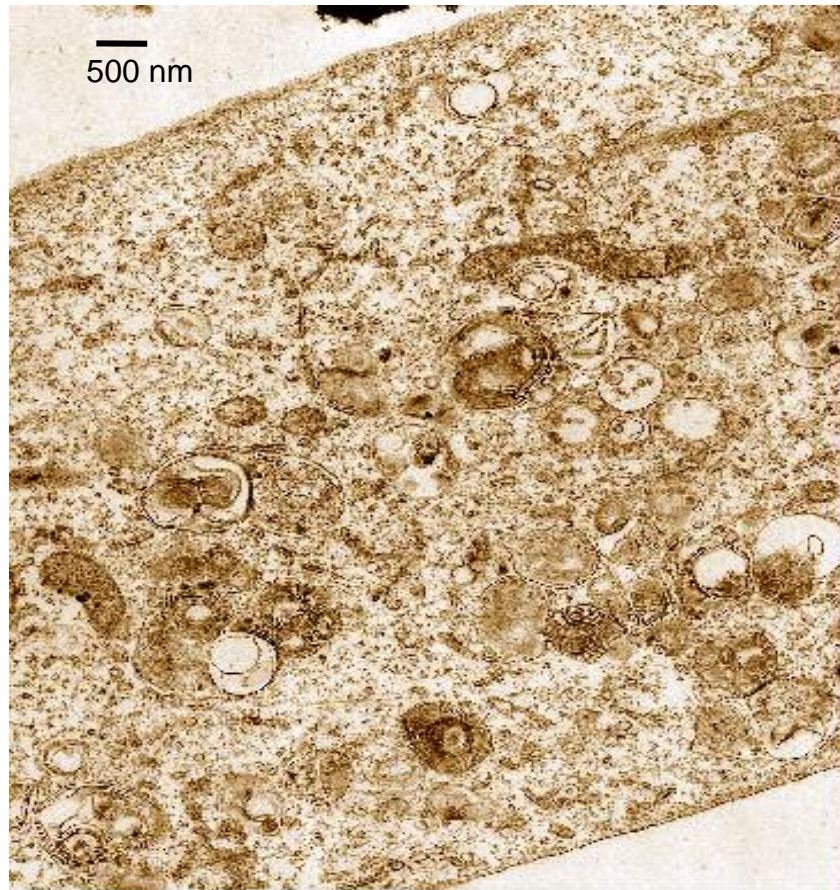


Figure 1. Transmission electron microscope image of prostate carcinoma cell cultured with untreated nanoparticles. There is no visible concentration of nanoparticles within the cell.

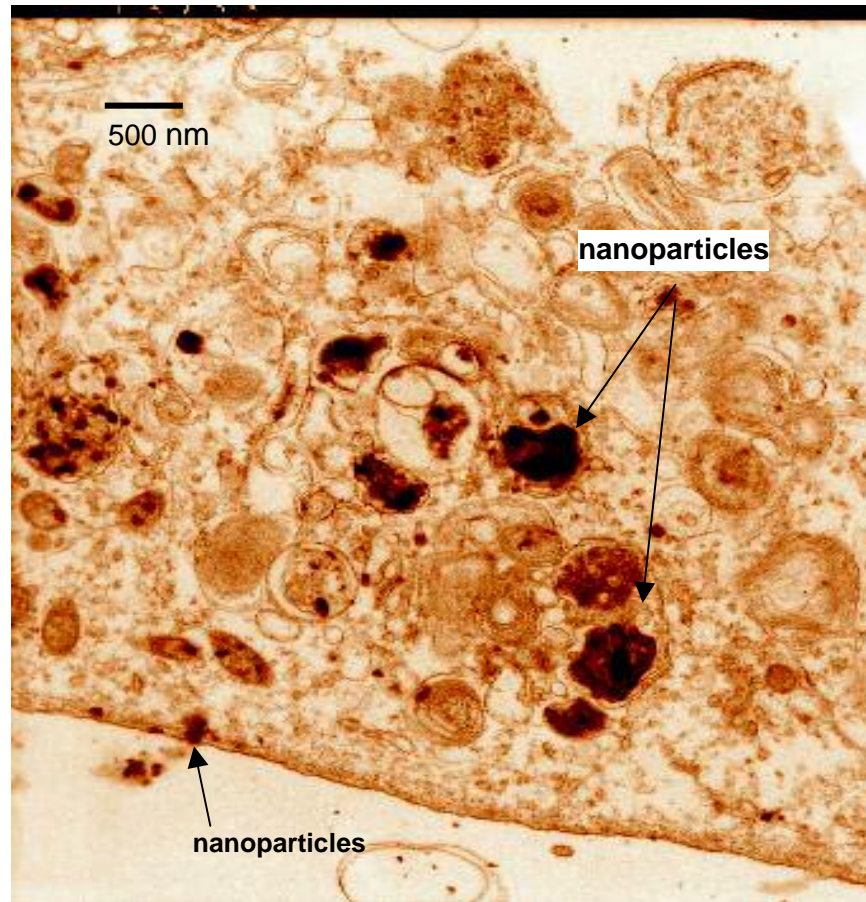


Figure 2a. Transmission electron microscope image of prostate carcinoma cell with gum arabic treated nanoparticles at the membrane surface and within cellular components (i.e. lysosomes, vacuoles). Cells were inoculated with the treated nanoparticles for 30 minutes.

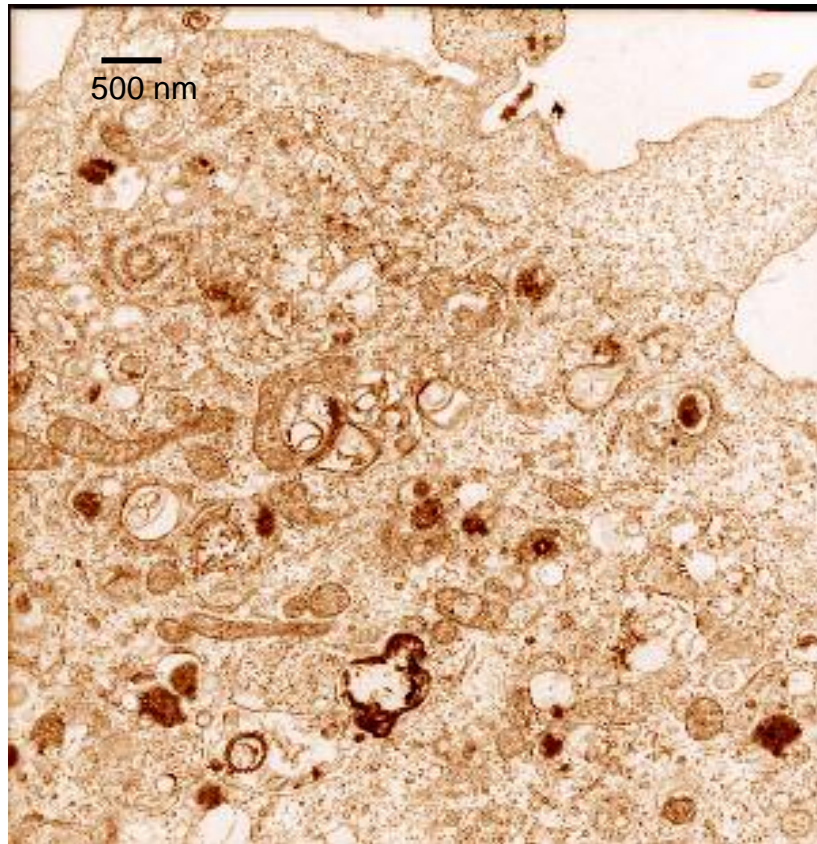


Figure 2b. Transmission electron microscope image of prostate carcinoma section with treated nanoparticles throughout the cell taken at a lower magnification.

Immunofluorescence studies also demonstrated that the FITC-labeled gum arabic nanoparticles were internalized by the cells. The cells were inoculated with the labeled particles for 24 hr. The fluorescent image (Figure 3b) highlights the cells that correspond to the cells in the phase image (Figure 3a). These images are representative of the entire glass slide on which the cells were cultured.

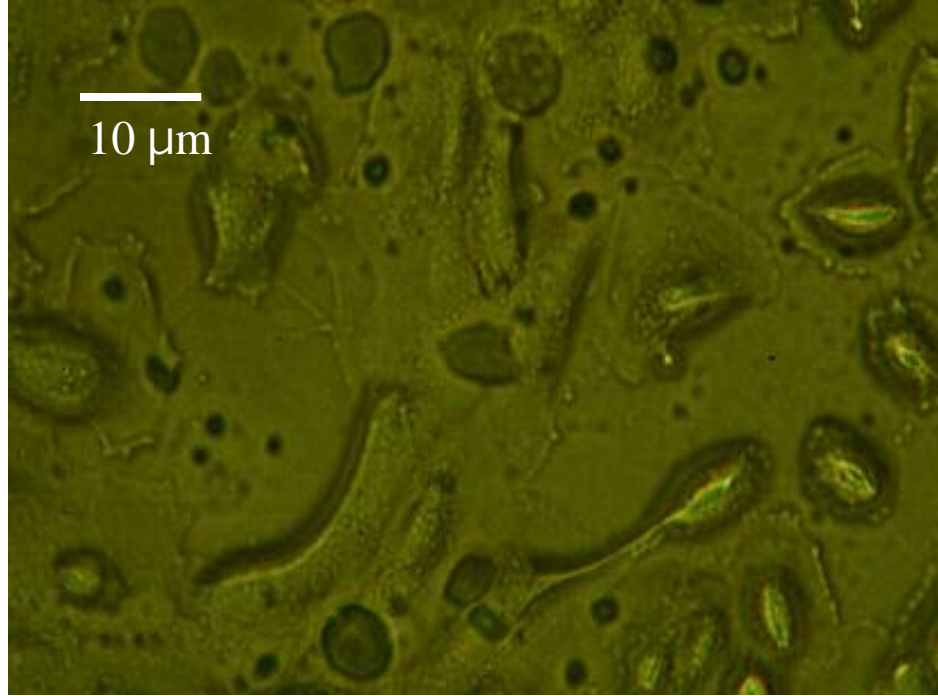


Figure 3a. Phase view of DU-145 cells grown on glass slides with fluorescently labeled gum arabic coated nanoparticles.

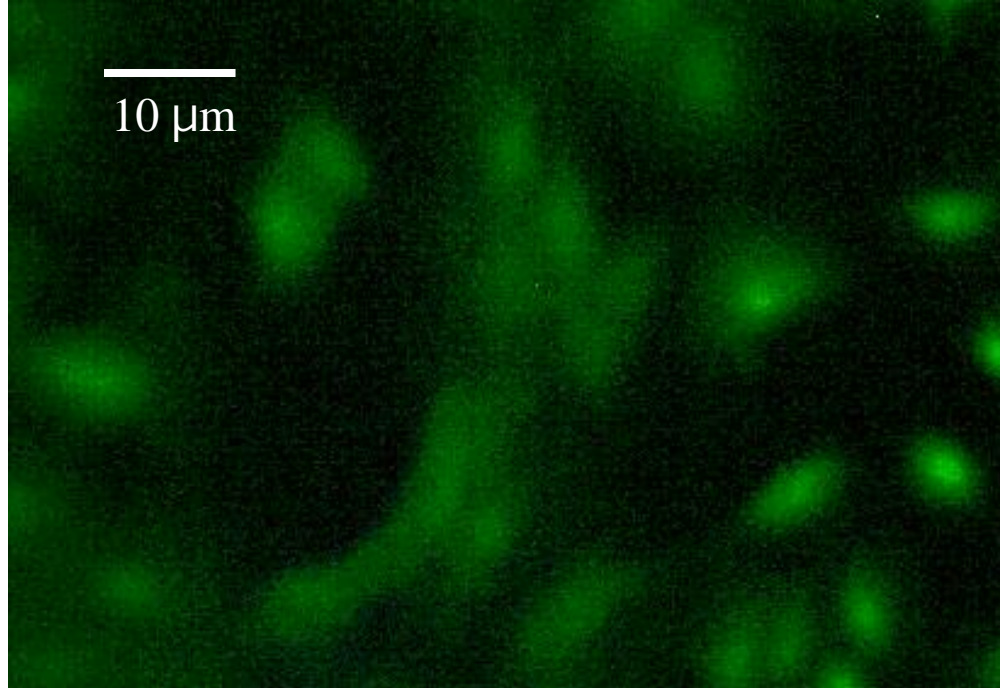


Figure 3b. Fluorescent image of DU-145 cells grown on a glass slide with FITC-labeled gum arabic coated nanoparticles

DAPI was used to differentiate between the nucleus of the cells and the cytoplasm, as well as a marker for cell viability. The homogenous color given off by the DAPI stained nuclei indicate that the cells from the control are healthy (Figure 4a). The experimental cultures show a significant difference in color, in that the nucleus is clearly stained and bright, but the cytoplasm is glowing a red hue (Figure 4b). The red hue is from TRITC-labeled nanoparticles coated with gum arabic. The contrast provided by TRITC and DAPI make it easier to differentiate between the regions of the cells that have internalized the nanoparticles. These results correlate well with the images taken from TEM, as well as the immunofluorescence studies.

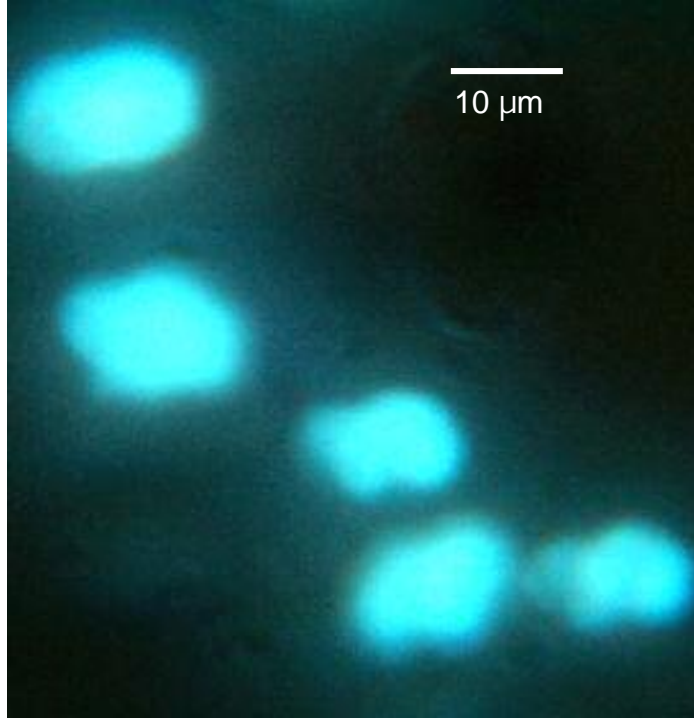


Figure 4a. DAPI stained nuclei of DU-145 cells (controls) without surface treated nanoparticles.

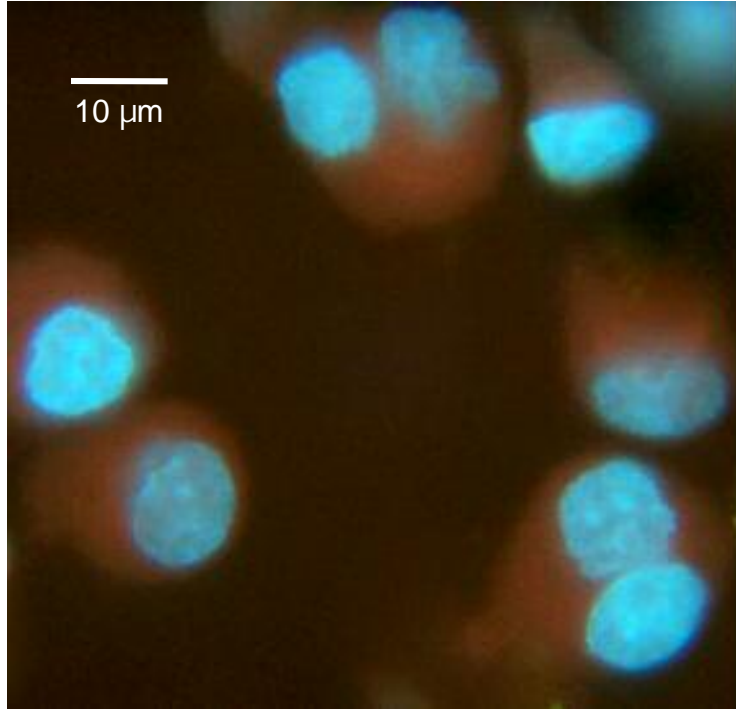


Figure 4b. Prostate carcinoma cells inoculated for 30 minutes with TRITC-labeled nanoparticles coated with gum arabic. DAPI stained nuclei (blue) for cell viability and to differentiate between nuclei and the cytoplasm (red) containing the nanoparticles.

#### 4.0 Discussion

Developing and finding materials for surface modification is critical to the fate of nanoparticles for use in biological applications. A number of studies have demonstrated that various types of surface treatments show a marked increase or decrease in internalization of magnetic nanoparticles, even with materials commonly used in medical applications (i.e. dextran) (Berry and Curtis 2003). It has also been determined that mammalian cells respond better to hydrophilic surfaces because they are more likely to resist opsonization and remain in circulation (Berry et al. 2003). In the case of polymer coatings, the role of polymers on nanoparticle stability can be complicated. According to literature, if added polymer moieties are polyelectrolytes, there will be a combination of electrostatic effects as well as effects that arise from the polymeric nature of the additive; this combined effect is referred to as electrostatic stabilization (Hiemenz and Rajagopalan 1997). One particular study hypothesized that electrostatic interactions govern adsorption of anionic nanoparticles onto the cell membrane (Wilhelm et al. 2003).

It is apparent from experimentation that gum arabic facilitates the internalization of the magnetic nanoparticles into prostate carcinoma cells. The treated nanoparticles were found in secondary lysosomes and vacuoles in the Golgi zones of the DU145 cells. The micrographs of the untreated nanoparticles show clear Golgi zones. From previous work not reported in chapter 4, it was determined that there is a strong physical adsorption of gum arabic onto the surface of the magnetite nanoparticles [Williams et al., 2004]. It has been postulated that the glycoprotein in gum arabic is capable of strong binding interactions due to the electrostatic attraction between a negatively charged group of a gum arabic molecule and a positively charged site on the oxide surface (Leong et al.

2001b). This would leave the hydrophilic carbohydrate blocks of the gum arabic molecule free in solution, which in turn, provides stabilization for the nanoparticles.

Cancer cells are notorious for having very high metabolisms and they have a need for high energy food sources. Gum arabic, being a complex polysaccharide/glycoprotein molecule, is an attractive food source and can potentially serve as a means to promote the uptake of nanoparticles into cancer cells. Gum arabic can also be labeled with various fluorescent probes by covalent labeling techniques. The protein molecules contain a sufficient amount of highly reactive amino groups on their surface. A wide variety of probes with different fluorescent properties containing protein reactive groups, such as isothiocyanate, carboxylic acid, succinimidyl ester, or sulphonyl halides are commercially available. Carbohydrates are less reactive and a limited number of reactive probes (isothiocyanates derivatives) can be used in waterfree organic solvents at elevated temperatures (van de Velde et al. 2003). It is important to point out that it is not clear whether the protein or carbohydrate groups of gum arabic were labeled with FITC in our experiments.

Another issue to address concerns the nanoparticles themselves. In order for the nanoparticles to effectively be internalized by the cells, the particles have to be on the order of single particulates. However, nanoparticles tend to form agglomerates during synthesis. Gum arabic prevented them from forming larger agglomerates in solution by providing steric stabilization. The solution of nanoparticles was polydispersed in size with an average agglomerate size of 100 nm (primary particle size equal to 6 nm) as opposed to 260 nm without gum arabic reported in Chapter 4. The agglomerates that were formed during synthesis might have prevented a significant amount of nanoparticles

from undergoing fluid phase endocytosis. In the case of the untreated particles, they were too large to be internalized by the cancer cells.

Using gum arabic to treat nanoparticles could benefit several biological applications. One obvious application is the detection of cancer cells, either *in vivo* or *in vitro*. Gum arabic might be effective in identifying cancerous cells in the blood stream or parts of the body to target regions plagued by tumors. Questions still remain whether coating with gum arabic will allow for specific interactions with cells of interest. In this case, it might be possible to tailor gum arabic by attaching a particular ligand or molecule that will catalyze a specific reaction (i.e. protein expression, apoptosis) and/or bind to specific cell types. The internalization of labeled magnetic nanoparticles within cells could lead to further applications, such as magnetic fluid hyperthermia or enhanced magnetic resonance imaging.

## **5.0 Conclusion**

We have demonstrated in this study that gum arabic contributed to the internalization of magnetic nanoparticles in prostate carcinoma cells. The process was rapid and most likely due to endocytosis. The untreated nanoparticles showed no visible internalization by the cells, indicating that surface modification can facilitate the interactions between nanoparticles and cells. As mentioned in other reported studies, it is important to understand the relationship between nanoparticles and cells prior to use in *in vivo* experimentation. This chapter provides an example of how critical surface properties are to the fate of nanoparticles in biological systems.

## CHAPTER 6 – CONCLUSIONS

It appeared as though the magnetic nanoparticles, like many other particles, formed agglomerates during synthesis from experimentation. According to literature, this phenomenon is a result of nanoparticles compensating for their high surface energies due to their large surface area to volume ratios. The primary particles were very small (less than 10 nm), but the agglomerates were on the order of 100 nm or greater. For biological applications, where size is a factor, this could impede delivery of material to cells.

Particle stability became another hurdle to overcome, particularly when dealing with physiological solutions because of agglomeration. Physiological solutions contain components, such as salts, proteins, and enzymes that can influence the surface characteristics of the particles and promote further agglomeration over a short or long period of time (depending on the concentrations of the components and surface properties of the nanoparticles). In a system where particles need to remain suspended (i.e. *E. coli* in batch culture), agglomeration can cause the nanoparticles to undergo sedimentation and fall out of solution. This limits the potential for nanoparticle/cell interactions.

Studies were performed to determine how nanoparticles affected the growth of microbial cells (*E. coli*) by studying cell cultures in the presence of several types of inorganic nanoparticles. In addition, understanding the colloidal properties of the inorganic nanoparticles was an important factor. Dynamic light scattering (DLS) and transmission electron microscopy (TEM) were used to quantify size distribution and determine morphology of the nanoparticles, respectively. It was evident from the results that the nanoparticles did not impose any toxic effects on *E. coli*. The nanoparticles did not show any significant concentrations on the membranes, and there was no evidence of

internalization of the nanoparticles within *E. coli*. This is because the particles were too agglomerated. There was no evidence of growth inhibition, although at higher concentrations the growth rates were slightly lower.

When the synthesized magnetic nanoparticles were treated with gum arabic, there was a drastic difference in colloidal behavior. Zeta potential analysis confirmed that surface modification using the natural polymer provided steric stabilization, preventing the particles from agglomerating and precipitating out of solution. The range in which the measurements fell for both treated and untreated particles indicated that the dispersions were unstable. From this, it was concluded that another force (steric hindrance) was acting on the particles to keep them from colliding into each other. The negatively charged molecules of gum arabic must repel each other, thus promoting particle stability. DLS measurements further support this conclusion as seen in the experimental results.

Gum arabic has a strong affinity toward the iron oxide surface, but there is a limit to how much will adsorb on the surface according to adsorption data. Adsorption for many polymers can occur by electrostatic, covalent, hydrophobic, and hydrogen bonding mechanisms. In the case of gum arabic, electrostatic attraction applies as the negatively charged groups of the gum arabic molecule bind to positive sites on the oxide surface. The Langmuir adsorption model has limitations, in that it assumes that the solid surface is homogenous, and coverage of the coating material is limited by a single monolayer (assuming the adsorbed molecules do not interact with each other). It is, however, quite possible that gum arabic is capable of multilayer adsorption because of its complex structure and charged functional groups.

It was demonstrated in this study that gum arabic promoted a favorable interaction between magnetic nanoparticles and prostate carcinoma cells. Gum arabic contributed to the internalization of magnetic nanoparticles, and the process was rapid and most likely due to endocytosis. The untreated nanoparticles showed no visible internalization by the cells, indicating that surface modification can facilitate the interactions between nanoparticles and cells. As mentioned in other reported studies, it is important to understand the relationship between nanoparticles and cells prior to use in in vivo experimentation. This paper provides an example of how critical surface properties are to the fate of nanoparticles in biological systems.

## CHAPTER 7– RECOMMENDATIONS FOR FUTURE WORK

There are additional areas to be studied concerning the impact of gum arabic on surface modification and nanoparticle/cell interactions. In terms of nanoparticle synthesis, the particles used during experimentation should be as small as possible to try and maximize internalization. Particles larger than the ones used in this paper are unlikely to undergo endocytosis. Cells, such as macrophages, are able to engulf larger macromolecules through a process known as phagocytosis. However, to exploit the properties of magnetism and large surface areas, the particles should be on the nanometer scale and agglomeration should be minimized.

There is much to learn about the properties of gum arabic as a material for treating materials. Gum arabic is a complex structure, and not all is understood about how it behaves in relation to solid surfaces. We know from this paper that it has a high affinity for oxide surfaces, and that it enables iron oxide nanoparticles to remain stable in aqueous solutions. An important study would be to determine if gum arabic drastically changes the properties of nanoparticles during synthesis. Like other polymers (i.e. polyvinyl alcohol) used in some chemical synthesis of materials, perhaps gum arabic could affect the size, surface properties, and crystallinity of the particles.

The use of gum arabic as a source for targeting cancer cells is a new and preliminary attempt to aid in finding more efficient medical therapies. There are still questions about how the treated particles enter the cells, how the cells recognize the gum arabic, and at what rate this process occurs. A study involving the inoculation of nanoparticles at time points shorter than 30 minutes will provide insight to the

endocytosis process. Several reports have described a design for measuring nanoparticle concentration per cell using a method known as magnetophoresis (a relationship between magnetic force and viscous force per unit length). This requires a magnetic field gradient and a microscope setup that will allow one to capture images of cell motion to calculate the velocity, thereby determining the number of particles per cell from the previously mentioned relationship. Another method would be to simply count the number of particles visible in a TEM micrograph image of cells, but this would be less accurate. One would need to know the thickness of the section, the dimensions of the cells, and the particles would have to clearly be in single particulate form.

Studies involving normal, healthy cells are necessary to determine if gum arabic is suitable for cancer therapies. Although cancer cells are more aggressive than normal cells, there needs to be clear results that show gum arabic treated particles are not internalized at the same rate by normal cells. Massive internalization by normal cells would defeat the purpose of using the material for various medical therapies. So in the case with prostate carcinoma cells, a study involving healthy prostate cells or surrounding tissue would contribute greatly to this research. Studies have reported that normal cells showed little interest in sugar-coated nanoparticles (James 2003). However, it is not clear at this point, whether gum arabic promotes specific or nonspecific interactions with cells.

Characterization of the treated particles after internalization may determine whether the gum arabic remains on the surface of the nanoparticles or is completely metabolized by the cells. Questions about how gum arabic affects the overall function of the cells may be answered by measuring the amount of gum arabic on the surface using

thermogravimetric analysis, for example. After experimentation, the cells would need to be lysed to remove the magnetic particles, separated either by magnet or centrifugation, and then analyzed for the presence of gum arabic. It is probable that cells may digest the gum arabic, leaving bare particles exposed to other components and organelles within the cytoplasm, and this could influence the overall integrity of the cells. A study of these components and their affinity toward the magnetic particle surface will aid in revealing the mechanisms involved in the migration of particles throughout cells.

## APPENDIX A – FITC/Gum Arabic Chemistry

Modified from protein labeling protocol outlined in the Handbook of Fluorescent Probes (Haugland, 2002).

- Combine 200  $\mu$ l dimethylformamide (DMF) with 1 mg fluorescein isothiocyanate (FITC).
- Add above to 1 ml 95 % ethanol to create a master solution.
- In a separate vial, combine 15 ml of 10 wt% gum arabic with 3 ml of phosphate buffer saline (PBS).
- From master solution, take 100  $\mu$ l and add dropwise to gum arabic- PBS solution (stirring).
- Let incubate for 1 hr on a gyratory shaker.
- In a 1.5 ml centrifuge tube, add 500  $\mu$ l ( $2.35 \times 10^{-5}$ g) nanoparticles.
- Add to the same centrifuge tube 500  $\mu$ l of labeled gum arabic solution.
- Sonicate with a sonicating tip for 1 minute, then centrifuge @ 18,000 rpm for 10 minutes.
- Remove supernatant, add 500  $\mu$ l of deionized water, re-sonicate and centrifuge (repeat this step 3 times to assure removal of excess gum arabic).

## APPENDIX B – TRITC Labeled Nanoparticles

\*Protocol modified from Imhof et al. 1999. *J. Phys. Chem.*, 103, 1408-15.

- Dissolve 0.0357 g tetramethylrhodamine isothiocyanate (TRITC) in 0.1827 g 3-(aminopropyl)triethoxysilane (APTS).
- Combine TRITC-APTS solution with 1.30 ml anhydrous ethanol and allow reaction for 12 hrs on a gyratory shaker.
- Remove 390  $\mu$ l of TRITC-APTS-ethanol solution and add to 5 ml solution of iron oxide nanoparticles suspended in ethanol.
- Allow reaction for 24 hrs on a gyratory shaker.
- Centrifuge and wash several times to remove excess APTS-TRITC.

## REFERENCES

- <http://www.geosci.ipfw.edu/XRD/techniqueinformation.html>.
- Alper J. 2003. Turning sweet on cancer. *Science* 301:159-160.
- Babes L, Denizot B, Tanguy G, Le Jeune JJ, Jallet P. 1999. Synthesis of iron oxide nanoparticles used as MRI contrast agents: a parametric study. *J. Coll. Inter. Sci.* 212:474-82.
- Bandyopadhyaya R, Nativ-Roth E, Regev O, Yersushalmi-Rozen R. 2001. Stabilization of individual carbon nanotubes in aqueous solutions. *Nanoletters* 2(1):25-28.
- Berry C, Wells S, Charles S, Curtis ASG. 2003. Dextran and albumin derivatised iron oxide nanoparticles influence on fibroblasts in vitro. *Biomaterials* 24:4551-4557.
- Berry CC, Charles S, Wells S, Dalby MJ, Curtis ASG. 2004. The influence of transferrin stabilised magnetic nanoparticles on human dermal fibroblasts in culture. *Int. J. Pharma.* 269:211-25.
- Berry CC, Curtis SG. 2003. Functionalisation of magnetic nanoparticles for applications in biomedicine. *J. Phys. D: Appl. Phys.* 36:R198-R206.
- Bruchez M, Moronne M, Gin P, Shimon W, Alivisatos AP. 1998. *Science* 281:2013-15.
- Byers CH, Harris MT, Williams DF. 1987. *I&EC Research* 26(9):1916-23.
- Chan WCW, Nie S. 1998. *Science* 281:2016.
- Chouly C, Pouliquen D, Lucet I, Jeune JJ, Jallet P. 1996. *Microencapsulation* 13(3):245-55.

- Coates.J. 2000. Interpretation of infrared spectra: a practical approach. Encyclopedia of Analytical Chemistry:10815-10837.
- Couvreur P, Dubernet C, Puisieux F. 1994. Eur. J. Pharm. Biopharm 41(1):2-13.
- Dickinson E. 2003. Hydrocolloids at interfaces and the influence on the properties of dispersed systems. Food Hydrocolloids 17:25-39.
- Douglas SJ, Davis SS, Illum L. 1987. Nanoparticles in drug delivery. CRC Critical Reviews in Therapeutic Drug Carrier Systems 3(3):233-254.
- Dural C. 1953. Inorganic Thermogravimetric Analysis. Amsterdam: Elsevier.
- Durig JR. 1980. Analytical Applications of FTIR of Molecular and Biological Systems. Dordrecht: D. Riedel.
- Ehrman S, Friedlander SK, Zachariah MR. 1999. J. Mat. Res. 14:4551-61.
- Fauconnier ML, Blecker C, Groyne J, Razafindralambo H, Vanzeveren E, Marlier M, Paquet M. 2000. Characterization of two acacia gums and their fractions using a langmuir film balance. J. Agric. Food Chem 48:2709-2712.
- Friedlander SK. 1977. Smoke, dust, and haze: Fundamentals of aerosol behavior. New York: Wiley.
- Gaur U, Sahoo SK, De TK, Ghosh PC, Maitra A, Ghosh PK. 2000a. Biodistribution of fluoresceinated dextran using novel nanoparticles evading RES. In. J. Pharma 202:1-10.
- Gaur U, Sahoo SK, De TK, Ghosh PC, Maitra A, Ghosh PK. 2000b. Biodistribution of fluoresceinated dextran using novel nanoparticles evading reticuloendothelial system. Int. J. Pharm 202:1-10.

- Graber KC, Freeman RG, Hommer MB, Naton MJ. 1995. Preparation and characterization of Au Colloid Monolayers. *Anal. Chem* 67:735-43.
- Haugland RP. 2002. Handbook of Fluorescent Probes and Research Products. Molecular Probes, editor.
- Hiemenz PC, Rajagopalan R. 1997. Principles of Colloid and Surface Chemistry. . editor. New York: Marcel Dekker, Inc.
- Islam AM, Phillips GO, Snowden MJ, Williams PA. 1997. A review of recent developments on the regulatory, structural, and functional aspects of gum arabic. *Food Hydrocolloids* 11(4):493-505.
- James K. 2003. Nanoparticles fight cancer with lethally high 'fever'. *Small Times*.
- Jordan A, Scholz R, Wust P, Schirra H, Schiestel T, Schmidt H, Felix R. 1999. Endocytosis of dextran and silan-coated magnetite nanoparticles and the effect of intracellular hyperthermia on human mammary carcinoma cells in vitro. *J. Magnetism and Magnetic Materials* 194:185-96.
- Kim DK, Zhang Y, Voit W, Rao KV, Muhammed M. 2001a. Synthesis and characterization of surfactant-coated superparamagnetic monodispersed iron oxide nanoparticles. *J. Magnetism and Magnetic Materials* 225:30-36.
- Kim DK, Zhing Y, Voit W, Rao KV, Muhammad M. 2001b. *J Mag Mag Mat.* 225:30-36.
- Kreuter J. 1997. Colloidal Drug Delivery Systems. New York: Marcel Dekkar.
- Leong YK, Seah U, Chu SY, Ong BC. 2001a. Effects of gum arabic macromolecules on surface forces in oxide dispersions. *Colloids and Interfaces* 182:263-68.
- Leong YK, Seah U, Chu SY, Ovy BC. 2001b. *Colloids and Surfaces A* 182:263-68.

- Lin C, Yang Y, C. C, Chen G, Chen CC, Wu Y-C. 2002. Selective Binding of Mannose-Encapsulated Gold Nanoparticles to Type 1 Pili in E. coli. *J. Am. Chem.Soc.* 124:155-68.
- Ma M, Zhang Y, Yu W, Shen H, Zhang H, Gu N. 2003. Preparation and characterization of magnetite nanoparticles coated by amino silane. *Colloids and Surfaces A: Physichem. Eng. Aspects* 212:219-26.
- Massart R. 1981. Preparation of aqueous magnetic liquids in alkaline and acidic media. *IEEE Transactions on Magnetics* 17(2):1247-48.
- Moghimi SM, Hunter AC, Murray JC. 2001. Long-circulating and target-specific nanoparticles: Theory to practice. *Pharm Rev.* 53:283-318.
- Moore A, Marecos E, Bogdanov A, Weissleder R. 2000. Tumoral distribution of long-circulating dextran-coated iron oxide nanoparticles in a rodent model. *Radiology* 214:568-74.
- Moreno R. 1992. *American Ceramic Society* 7:1647.
- Morrish AH. 2001. *The Physical Principles of Magnetism*. New York: IEEE Press.
- Pankhurst QA, Connolly J, Jones SK, Dobson J. 2003. Applications of magnetic nanoparticles in biomedicine. *J. Phys. D: Appl Phy.* 36:R167-181.
- Phillipse AP, van Bruggen MPB, Pathmamanoharan C. 1994. Magnetic silica dispersions: preparation and stability of surface-modified silica particles with a magnetic core. *Langmuir* 10:92-99.
- Poortinga AT, Bos R, Norde W, Busscher HJ. 2002. Electrical double layer interactions in bacterial adhesion to surfaces. *Surface Science Reports* 47:1-32.

- Pouliquen D, Perroud H, Calza F, Jallet P, Le Juene J. 1992. Magnetic Resonance in Medicine 24:75-84.
- Prozorov T, Kataby G, Prozorov R, Gedanken A. 1999. Effect of surfactant concentration on the size of coated ferromagnetic nanoparticles. Thin Solid Films 340:189-193.
- Ray AK, Bird PB, Iacobucci A, B.C. Clark J. 1995. Functionality of gum arabic: Fractionation, characterization, and evaluation of gum fractions in citrus oil emulsions and model beverages. Food Hydrocolloids 9(2):123-31.
- Shinkai M. 2002. Functional magnetic particles for medical application. J. Bioscience and Bioeng. 94(6):606-613.
- Tischer CA, Gorin PAJ, Iacomini M. 2002. The free reducing oligosaccharides of gum arabic: aids for structural assignments in the polysaccharide. Carbohydrate Polymers 47:151-158.
- van Blaaderen A, Vrij A. 1992. Langmuir 8:2921-31.
- van de Velde F, Weinbreck F, Edelman MW, van der Linden E, Tromp RH. 2003. Visualisation of biopolymer mixtures using confocal scanning laser microscopy (CSLM) and covalent labeling techniques. Colloids and Surfaces B: Biointerfaces 31:159-68.
- Velikov KP, Zegers GE, Bladderer Av. 2003. Synthesis and characterization of large colloidal silver particles. Langmuir 19:1384-1389.
- Wilhelm C, Billotey C, Roger J, Pons JN, Bacri J-C, Gaxeau F. 2003. Intracellular uptake of anionic superparamagnetic nanoparticles as a function of their surface coating. Biomaterials 24:1001-1011.

Yudin IK, Nikolaenko GL, Kosov VI, Agayan VA, Anisimov MA, Sengers JV. 1997. A compact photon-correlation spectrometer for research and education.1-23.

Zhang Y, Kohler N, Zhang M. 2001. Intracellular uptake of polyethylene glycol and folic acid modified magnetite nanoparticles. Mat. Res. Soc. Symp. Proc. 676:y9.8.1-y9.8.5.